A STUDY OF INFRARED PRINCIPLES WITH EMPHASIS ON THERMAL DETECTION

by

Atanur Demirelli

Thesis Supervisor:

Prof. Dr. Necmi Tanyolaç

Robert College

School of Engineering

1969

ACKNOWLEDGMENTS

I would like to express my deep gratitude to Prof. Dr. N. Tanyolaç for his guidance and encouragement in the preparation of this work.

Special thanks are expressed to the Staff of Experimental Physics Division, Çekmece Research Center; in particular to Dr. A. Ferendeci for providing the necessary facilities and materials used in experimentation and to E. Yılmaz for his help on practicle details.

Finally, I would like to extend my thanks to "AR-GE Dairesi Başkanlığı" for lending some of their documents on the subject, and also to Messrs. C. Gül and E. Göktuna for their help and suggestions in experiments.

December, 1969 A. Demirelli

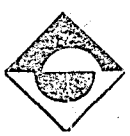

ABSTRACT

A survey of infrared principles is given in an attempt to determine the factors effecting the performance of infrared detection system. Various detection phenomena are discussed in a comparative manner. A full treatment of thermal detection theory is given. Possible experimental procedures are investigated for the construction of thermally sensitive materials.

Although an effective experimental procedure cannot be developed with the present facilities, the use of vacuum deposition is shown to give satisfactory results if certain provisions are made.

CONTENTS

I. THE NATURE OF INFRARED RADIATION

All types of radiation observed in nature are included in an electromagnetic spectrum which may be defined as the ordered arrangement of radiation according to wavelength, frequency, or energy criteria. There is no single source or detection mechanism that is useful over the entire range of this spectrum. Consequently, the electromagnetic spectrum has been separated into rather loosely defined spectral regions. The bases for these broad subdivisions are in accordance with the various means of generating, isolating, and detecting the radiations involved.

The following diagram shows the distribution of various spectral regions within the electromagnetic spectrum:

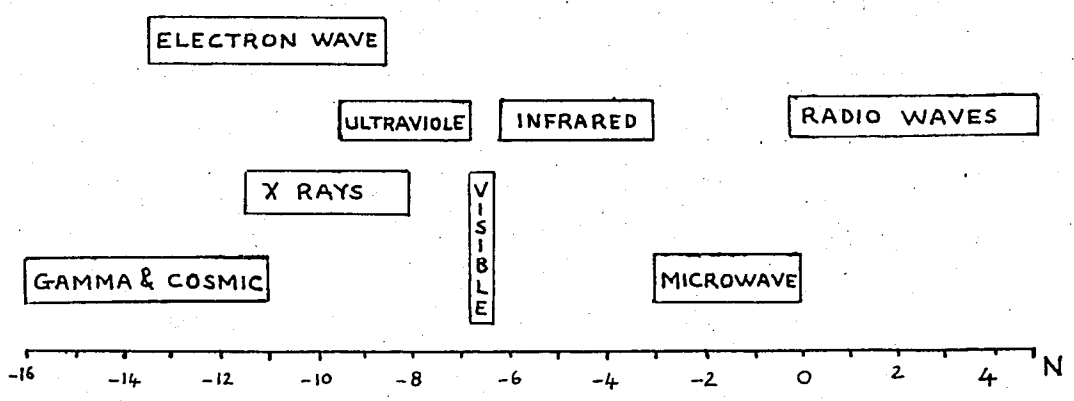

Wavelength: 10^{N} meters

Figure 1: Electromagnetic spectrum(1)

Infrared radiation lies between visible and microwave regions of the electromagnetic spectrum. Its limits are usually accepted as extending from 0.75μ to 1000μ of wavelength. For convenience in analysis, the infrared region is further subdivided into the following parts:

Near Infrared: 0.75μ- 1.5μ
Intermediate Infrared: 1.5μ - 6.0μ
Far Infrared: 6.0μ - 1000μ

It should be emphasized that these definitions are somewhat arbitrary, since observations show various overlapings between different regions. This statement applies especially to the separation of far infrared and microwave frequencies. Measurements are now being made with microwave electronics down to about 600μ of wavelength.

All the radiations defined in the electromagnetic spectrum have an important property in common: They all travel with the speed of light in vacuum, and may be considered as transporters of energy. However, in their mode of excitation and in the manner in which they interact with matter, they differ widely. Energies of the order of a billion electron-volts are associated with x-rays, whereas the far end of the microwave region transports only about a few micro-electron-volts. Another distinction related to different types of radiation is the method of generation applicable. Of the two neighbors of infrared in the electromagnetic spectrum, microwaves are generated by means of tuned electrical circuits, whereas visible and ultraviolet radiations are generated by electronic transitions and molecular vibrations within the atoms and molecules of the radiating source. Since the infrared lies in between visible and microwave

regions, it possesses characteristics common to both.

In principle, all matter above absolute zero of temperature ($0^{\circ}K$ or $-273^{\circ}C$) generates infrared radiation. This is why heated bodies provide excellent sources of infrared. Although all electromagnetic radiation produces heat when absorbed by matter, the infra red (IR) region can be more readily detected by the heat it produces. We must be very careful however, to distinguish between "heat waves" and the thermal radiation generated by an infrared source. "Heat waves" are transmitted by conduction and convection through physical media. On the other hand, the infrared radiation generated by a hot body does not require a physical medium for its transmission. It can be transmitted through vacuum as well as physical media and propagates in accordance with the laws of electromagnetic theory, travelling with the speed of light in vacuum, in common with all other forms of electromagnetic radiation.

Historically, the identification of thermal radiation as a form of electromagnetic radiation became possible after a series of scientific developments terminating with the emergence of Quantum Mechanics. We will indicate below, the basic steps of development which IR technology has undergone during the last two centuries. This should throw more light on the implication of the general phenomena of Infrared Radiation:

Infrared radiation was discovered by Sir William Herschel in 1800, during a series of experiments investigating the heating power among various colors in the solar spectrum. Herschel observed that the heating effect increased towards the red end of

the spectrum and did not reach a maximum until the limits of visible light were extended. Although Herschel and his followers showed that thermal radiation obeyed the laws of optics, the association of this radiation with light, was disputed for several decades. The identity of infrared with light became generally accepted after the works of Forbes who showed that heat radiation can be polarized in the same manner as light (1834), and after Fizean and Foucault who determined the wavelength of near infrared waves from interference fringes (1837).

In 1865 Maxwell predicted theoretically the existence of electromagnetic waves and proposed the identity of these waves with light waves. H. Hertz in 1887, produced electromagnetic waves in the laboratory, and confirmed that they propagate with the same velocity as light and have the same polarization properties. This chain of developments was terminated by Nichols and Tear in 1923, who succeeded in generating far infrared waves of 220 μ wavelength by means of a miniature spark oscillator similar to that used by Hertz, thus establishing that infrared radiation is of an electromagnetic nature.

Several attempts were made to determine the spectral distribution of radiation from a heated body. W. Wien and Lord Rayleigh attempted to derive the radiation law according to Classical Electromagnetic theory, but their predictions disagreed sharply with experimental facts. The correct solution to this problem was obtained through Planck's Hypothesis that the proper distribution of energy among the elementary oscillators composing the thermally radiating body can be obtained only if the concept of continuously divisible energy is abondoned (1900). The concept of discrete

energy levels, or the quantization of energy, was an approach which correctly predicted the spectral distribution of energy contained in black-body radiation. Maxwell stated that the energy states of elementary oscillators can vary only by integral multiples of elementary quanta($h\nu$), proportional to frequency. He also established the correct numerical value of the proportionality constant (h), now called Planck's Constant.

A. Einstein made the first important use of the quantum concept in the discovery of Phoelectric effect and established the idea of light quanta. The assumption that light consists of a bundle of photons defined by an energy proportional to frequency, gave accurate results for the Photoelectric effect. The description of light intensity by the number of photons passing through a given cross section, however, suggests that light possesses a Corpuscular nature. On the other hand, the corpuscular theory of light is inadequate in explaining the phenomena of interference and diffraction and one has to resort to wave phenomena to explain these effects.

We are thus faced with a duality; light behaves both as a wave, and a particle depending on the set of experiments performed. It is presently accepted that the phenomena related with the propagation of light are best described by the wave theory, while the intraction of various forms of electromagnetic waves with matter are best described by the corpuscular theory. The connecting link between the two theories lies in the fundamental postulate of Quantum Theory as stated by,

$$E = h\nu$$

and the de Broglie hypothesis which states that a wavelength is associated with every particle of mass (m), according to the relation

$$\lambda = \frac{h}{mv}$$

where (v) is the velocity of the particle and $(p = mv)$ is its momentum.

The "matter waves" described by this relation would have extremely short wavelengths, unobservable for macroscopic objects. However, the length of the waves are comparable to the dimensions of the particle for bits of matter as small as an electron, as can be verified by substituting representative values for the momentum.

II. INFRARED SOURCES

A. THE PHENOMENA OF EMISSION AND ABSORBTION.

The main sources of radiation in the visible and infrared regions of the spectrum fall into one of the following three classes:

(1) Thermally excited solids giving a continuous spectrum of radiation.

(2) Excited gases giving a series of emission lines.

(3) Luminescent materials, which are in general optically excited solids, giving line or band spectra.

Sources of the first class are the most common, due to their continuous radiation extending indefinitely into the infrared region.(2) Most emission spectra of excited gases show weak lines in the infrared.

In the treatment of emission and absorbtion phenomena, it is convenient to define an ideal radiator and absorber of radiation, called a black body. This is simply a body which absorbs all the radiation incident on it. If such a body were to be placed inside a uniform temperature enclosure, it would come to thermal equilibrium at the temperature of the enclosure. Under these conditions, the body will emit just as much radiation as it absorbs for any wavelength. It will be shown later in this section that a black body will emit a continuous spectrum for any temperature T. For

black bodies, the absolute temperature of the radiating object, the wavelength of the most intense radiation emitted, the radiation intensity as a function of wavelength, as well as the total radiated energy, are related with a fundamental radiation law called Planck's Law. Before attempting to derive this law, it is convenient to define the radiation terms that will be used during the development of the subject. These definitions are given below:

Radiant Power (P, watts): The radiant energy emitted by or incident upon a surface per unit time.

Radiant Intensity (E, watts/steradian): The radiant power emitted by a source into a unit solid angle.

Radiant Emittance (R, watts/m^2): Radiation power emitted by unit area of the source into an entire hemisphere.

Radiance (R_w, watts/m^2/steradian): The radiation power emitted by unit area of the source into a unit solid angle.

Irradiance ($\mathcal{H}$, watts/m^2): The radiation power incident on unit area of a surface.

Reflectivity (ρ): Fraction of incident radiation power which is reflected by a surface.

Absorbtivity (α): Fraction of incident radiation power which is absorbed by a surface.

Transmissivity (τ): Fraction of incident radiation power which is transmitted by the medium.

Emissivity (ϵ): A ratio which compares the radiating capacity of a surface to that of a black body. The value of ϵ for a black body is unity by definition.

If the above quantities are being considered at a given wavelength or wavelength interval, the subscript λ will be added.

The three numerical constants ρ, α, τ are not independent from each other. The Principle of Conservation of energy requires that the sum of absorbed, reflected and transmitted powers should be equal to the incident radiant power. This statement may be expressed as:

$$P_i = P_\alpha + P_\rho + P_\tau$$

Dividing both sides of this equation by P_i, we get

$$1 = \frac{P_\alpha}{P_i} + \frac{P_\rho}{P_i} + \frac{P_\tau}{P_i}$$

or, $$1 = \alpha + \tau + \rho \qquad (1)$$

Since the black body is defined as a perfect absorber and emitter, $\alpha = \epsilon = 1$ for a black body. In practice, a body will absorb only a fraction of the radiation falling on it, i.e. $R = \alpha \mathcal{H}$ and this fraction depends on wavelength. It should be noted here that color differences are based on absorbtion characteristics of different materials. During daylight for example, different bodies at room temp ($300^\circ K$) are continuously receiving radiation from the sun which is at an effective temperature of $6000^\circ K$.

These bodies are subject to a temperature difference and thus cannot emit the same wavelengths as they absorb. As a result, each body is observed in a different color, depending upon the wavelengths it absorbs.

The theoretical characteristics of a black body are very nearly approached by a uniformly heated cavity made from an opaque material. If the walls of such a cavity are held at a uniform temperature, the absorbtion and emission rates will be the same for both the inner and outer suffaces of the enclosure, as seen in the diagram below:

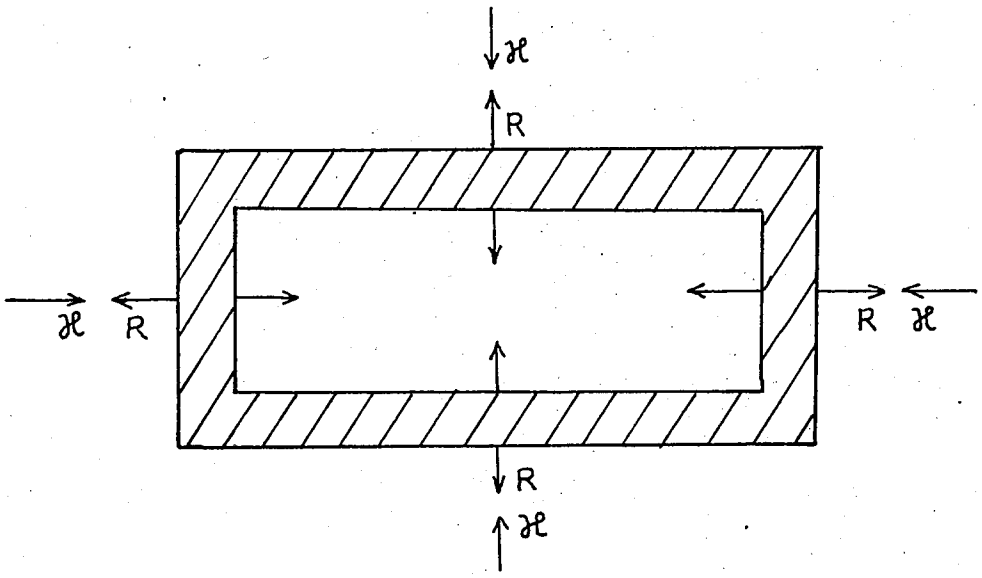

Figure 2: Cavity Radiation, $R = \mathcal{H}$.

The energy density of the electromagnetic field established in the cavity may be determined by a quantum mechanical analysis. Electromagnetic radiation is confined within the walls of the cavity so that its behavior may be described by a wave function which should reduce to zero at the boundaries.

Since the waves will be reflected back on themselves under these conditions, we know beforehand that a standing wave pattern will exist inside the cavity. The cavity should possess a large number of modes of oscillation, the frequencies of which are defined by the dimentions of the enclosure. These modes of

oscillation will be given by the solution of the wave equation under boundary conditions mentioned above. For simplicity, we can assume a rectangular enclosure with each side equal to L. The wave equation is given by:

$$\nabla^2\phi = \frac{1}{v^2}\frac{\partial^2\phi}{\partial t^2} \qquad (2)$$

where v is the velocity of waves set up in the cavity. Time variations may be taken into account by defining a new function ψ such as that

$$\phi = \psi e^{j\omega t} \qquad (3)$$

where ω is the angular frequency. We then get the time-independent wave equation,

$$\nabla^2\psi + \frac{\omega^2}{v^2}\psi = 0 \qquad (4)$$

$$\frac{\omega^2}{v^2} = \frac{(2\pi f)^2}{(\lambda f)^2} = \frac{4\pi^2}{\lambda^2}$$

where $\frac{1}{\lambda^2} = \frac{p^2}{h^2} = \frac{2mE}{h^2}$, by de Broglie relation.

so $\frac{\omega^2}{v^2} = \frac{8\pi^2 m E}{h^2}$

By substituting this, in equation (4), we obtain the wave-particle equation for the cavity, or the Schroedinger equation:

$$\nabla^2\psi + \frac{8\pi^2 m E}{h^2}\psi = 0 \qquad (5a)$$

This equation can be solved by separation of variables such that,

$$\psi(x,y,z) = X.Y.Z$$

$$YZ\frac{\partial^2 X}{\partial x^2} + XZ\frac{\partial^2 Y}{\partial y^2} + YX\frac{\partial^2 Z}{\partial z^2} = -\frac{8\pi^2 mE}{h^2}XYZ$$

$$\frac{1}{X}\frac{\partial^2 X}{\partial x^2} + \frac{1}{Y}\frac{\partial^2 Y}{\partial y^2} + \frac{1}{Z}\frac{\partial^2 Z}{\partial z^2} = -\frac{8\pi^2 mE}{h^2} \qquad (5b)$$

Since the sum of the three differential terms on the left side of this equation is a constant, each term should be equal to a constant. It is convenient to define these constants as follows:

$$\frac{1}{X}\frac{\partial^2 X}{\partial x^2} = -k_x^2$$

$$\frac{1}{Y}\frac{\partial^2 Y}{\partial y^2} = -k_y^2 \qquad (5c)$$

$$\frac{1}{Z}\frac{\partial^2 Z}{\partial z^2} = -k_z^2$$

so that we have the separate solutions as,

$$X = C_x \cos k_x x + D_x \sin k_x x$$

$$Y = C_y \cos k_y y + D_y \sin k_y y \qquad (6)$$

$$Z = C_z \cos k_z z + D_z \sin k_z z$$

Also, from equations (5b) and (5c) the relation among the constants is given by:

$$k_x^2 + k_y^2 + k_z^2 = \frac{8\pi^2 mE}{h^2} \qquad (7)$$

The components of ψ should each satisfy the boundary conditions separately, or,

$$X, Y, Z = 0 \quad : x, y, z = 0, L$$

The boundary conditions on X require that,

$$0 = C_x \cos(0) + D_x \sin(0), \text{ or } C_x = 0$$

$$0 = D_x \sin k_x L, \text{ or } \sin k_x x = 0$$

Thus, $k_x = \frac{n_x \pi}{L}$

Similarly, $k_y = \frac{n_y \pi}{L}$

$k_z = \frac{n_z \pi}{L}$ where $n_x, n_y, n_z = 0, 1, 2, 3, \ldots\ldots$

The solution of the wave equation (5) can now be expressed in terms of the set of integers (n_x, n_y, n_z), by substituting k_x, k_y, k_z in equation (6).

$$\psi = \psi_0 \sin \frac{n_x \pi}{L} \cdot \sin \frac{n_y \pi}{L} \cdot \sin \frac{n_z \pi}{L} \qquad (8)$$

where, $\psi_0 = D_x D_y D_z$

Each set of integers (n_x, n_y, n_z) yields an independent solution of the wave equation, and thus defines a unique mode of oscillation. If we substitute the values of k_x, k_y, and k_z into equation (7), we get,

$$n_x^2 + n_y^2 + n_z^2 = \frac{8mL^2}{h^2} E \qquad (9)$$

The quantity $(2mE)$ can be identified as the square of the momentum (p) of a particle. Using this fact, and the de Broglie relation between momentum and wavelength, equation (9) may be written in the form

$$n_x^2 + n_y^2 + n_z^2 = \frac{4L^2}{\lambda^2} \qquad (10)$$

Equation (10) states that the locus of points n_x, n_y, n_z is a sphere with radius $\frac{2L}{\lambda}$. Every single mode of oscillation is defined by a point $p(n_x, n_y, n_z)$ on the sphere, as shown below:

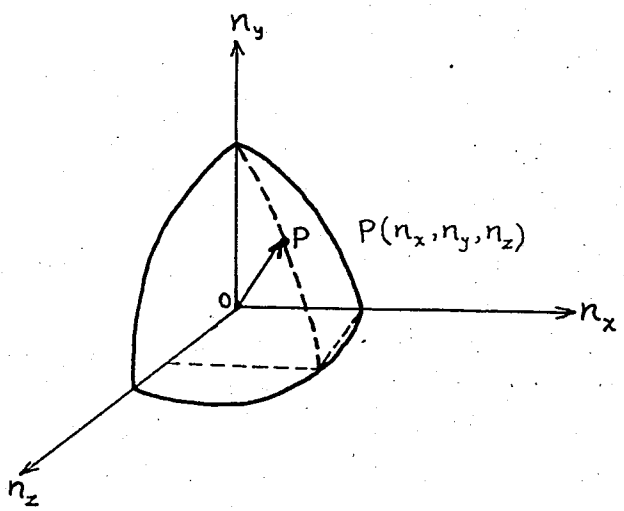

Figure 3: Sphere Locus

We are concerned with positive values of (n_x, n_y, n_z) so that the modes of oscillation for the system are represented by points lying within one octant of the sphereical surface defined by Equation (10). The total number of such points depends on the radius

of the sphere and therefore on the wavelength. The energy associated with a mode of oscillation (n_x, n_y, n_z) is expressed by Equation (9). For a macroscopic box with dimensions in the centimeter range, the energy spacing between any two modes, is in the order of 10^{-15} eV(3), as can be verified from Equation (9). We may thus treat the discrete points in Figure (3) as an approximate continuum, in which case the total modes of oscillation up to a given wavelength would be the volume of <u>one octant</u> of a sphere with radius $\frac{2L}{\lambda}$.

If N denotes the number of modes of oscillation, we have:

$$N = \frac{1}{8} \cdot \frac{4\pi}{3} \left(\frac{2L}{\lambda} \right)^3 = \frac{4\pi L^3}{3\lambda^3}$$

The density of such modes, or N per unit volume of the box would then be:

$$N_v = \frac{4\pi}{3\lambda^3} \qquad (11)$$

Within a wavelength interval $d\lambda$, the possible modes are given by the derivative of the above equation with respect to λ, or

$$|dN_v| = \frac{4\pi}{\lambda^4} d\lambda \qquad (12)$$

Remembering that electromagnetic waves are transverse, and have two possible states of polarization for each mode, Equation (12) becomes:

$$|dN_v| = \frac{8\pi}{\lambda^4} d\lambda \qquad (13)$$

We have determined the number of modes of oscillation within a wavelength interval $d\lambda$. In order to get an expression for the energy density in the same interval, we have to know the average energy associated with a mode of oscillation.

To a first order of approximation, the probability of existance of an oscillation mode with energy E, is governed by classical Boltzmann statistics expressed as,

$$f(E) = A e^{-\frac{E}{kT}} \tag{14}$$

According to Planck's hypothesis, each oscillation mode is allowed to have an energy equal to an integral multiple of elementary quanta $h\nu$, so that $E = nh\nu$ denotes the energies available to the system. If we let N_o be the number of oscillation modes with zero energy, then the probability of existance of modes with energy $h\nu$ is given by $N_o e^{-h\nu/kT}$. Similarly, the probability of modes with energy $2h\nu$ is expressed by $N_o e^{-2h\nu/kT}$. From a statistical viewpoint, the total oscillation modes in the system will be:

$$N_T = N_o + N_o e^{-h\nu/kT} + N_o e^{-2h\nu/kT} + \cdots = \sum_{n=0}^{\infty} N_o e^{-nh\nu/kT} \tag{15}$$

In order to determine the average energy associated with a single oscillation mode, we have to find the total energy contained within the electromagnetic field inside the cavity. The lowest allowable energy is $h\nu$ so that the total energy may be written as:

$$E_T = h\nu N_o e^{-h\nu/kT} + 2h\nu N_o e^{-2h\nu/kT} + 3h\nu N_o e^{-3h\nu/kT}$$

or,

$$E_T = \sum_{n=1}^{\infty} nh\nu N_o e^{-nh\nu/kT} \tag{16}$$

The average energy for an oscillation mode is,

$$\bar{E} = \frac{E_T}{N_T} = \frac{h\nu \sum_0^\infty n e^{-nh\nu/kT}}{\sum_0^\infty e^{-nh\nu/kT}} \qquad (17)$$

In the above expression, the denominator is seen to constitute of a geometric series with a common ratio $e^{-h\nu/kT}$ so that,

$$\sum_{n=0}^{\infty} = e^{-nh\nu/kT} = \frac{1}{1 - e^{-h\nu/kT}} \qquad (18)$$

The numerator of Equation (17) is indentified as the derivative expression of the denominator with respect to $-h\nu/kT$; thus its sum is given by,

$$\sum_1^\infty n e^{-nh\nu/kT} = \frac{\partial}{\partial\left(-\frac{h\nu}{kT}\right)} \left[\frac{1}{1 - e^{-h\nu/kT}}\right] = \frac{e^{-h\nu/kT}}{\left(1 - e^{-h\nu/kT}\right)^2} \qquad (19)$$

Substituting the expressions (18) and (19) into Equation (17), we have:

$$\bar{E} = \frac{h\nu . e^{-h\nu/kT}}{1 - e^{-h\nu/kT}}$$

The average energy may be expressed in a more convenient form by dividing both the numerator and denominator by $e^{-h\nu/kT}$. We then get:

$$\bar{E} = \frac{h\nu}{e^{h\nu/kT} - 1} \qquad (20)$$

We now have the average energy of an oscillation mode, and the number of oscillation modes within a wavelength interval $d\lambda$; multiplying Equation (13) by Equation (20), the energy density within the cavity, or the spectral energy density U_λ, may be written as:

$$U_\lambda . d\lambda = \frac{8\pi}{\lambda^4} . \frac{h\nu}{e^{+h\nu/kT} - 1} d\lambda \qquad (21)$$

Equation (21) is an expression of the fundamental Radiation Law, or Planck's Law.

We have thus far treated the generation of black-body radiation within a uniformly heated cavity. The cavity model will also give the emittance characteristics of a black body if the cavity enclosure is allowed to have a small opening through which electromagnetic radiation can propagate outwards. It can be shown by integrating Equation (21) that the flow of energy per unit time through the opening, or the spectral radiant emittance of a black-body, is related to the energy density by the relation [4],

$$R_\lambda = \frac{1}{4} c U_\lambda \qquad (22)$$

where (c) is the speed of light. If we combine the above relation with Equation (21) and express the frequencies in terms of wavelength through $c = \nu\lambda$, we get,

$$R_\lambda . d\lambda = \frac{2\pi c^2 h}{\lambda^5 (e^{hc/\lambda kT} - 1)} . d\lambda \qquad (23)$$

Equation (23) is the form of Planck's Law for blackbody radiant emittance within a finite spectral interval. A plot of this relationship for a blackbody at a temperature of 1000°K is shown in Figure (4). The emission characteristics at temperatures lower and higher than 1000°K are also shown in this figure. The points corresponding to maximum radiant power, are joined together, giving a straight line for wavelengths below 100 μ. The locus of such points is in fact a hyperbola as defined by Wien's Law. This behavior is more clearly illustrated if the curves are extrapolated for longer wavelengths, into the far infrared. The curve depicts experimental measurements.

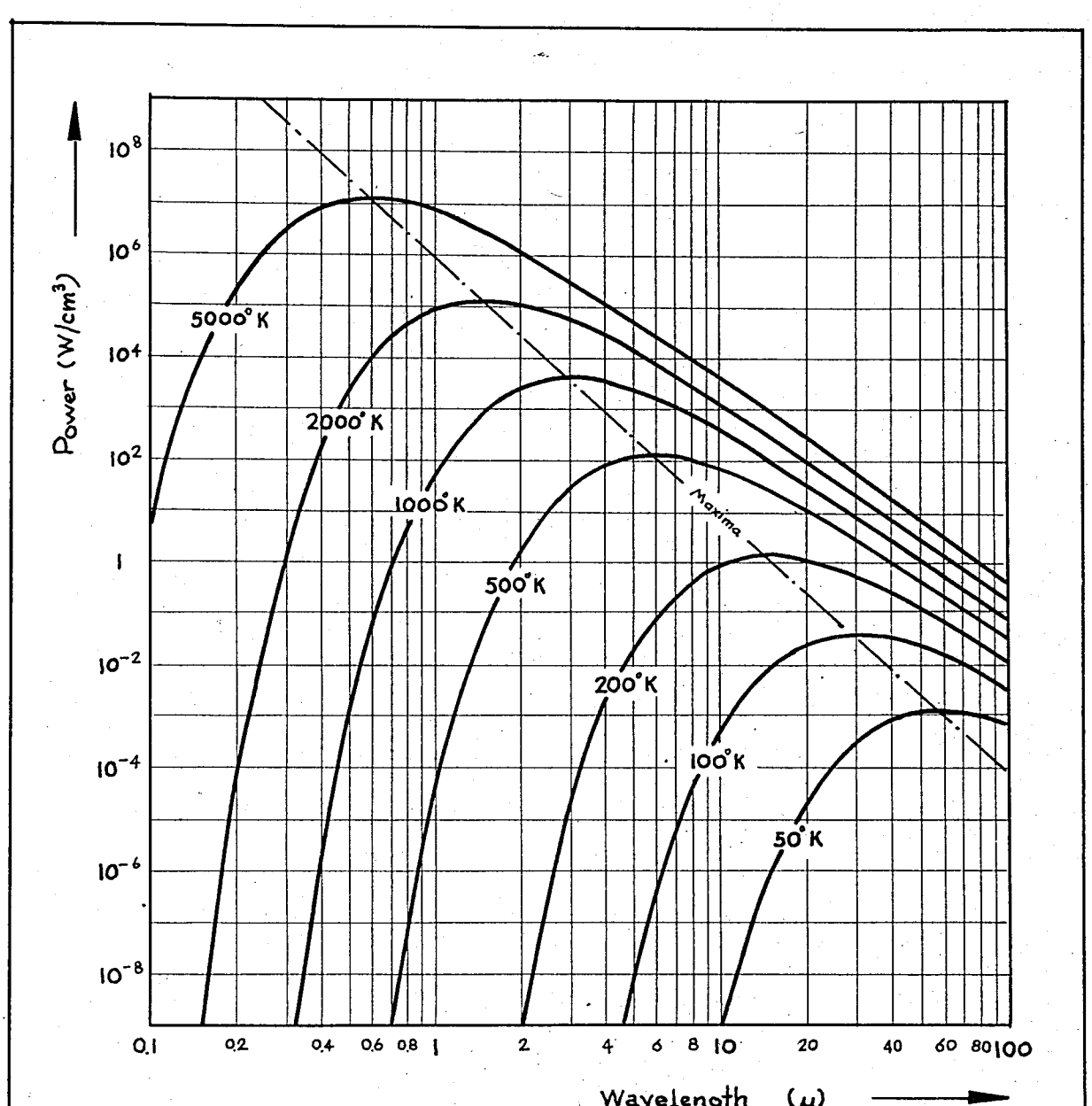

Fig. 4

Characteristics of
Blackbody Radiation

An expression for the number of photons emitted per unit time with a spectral interval $d\lambda$ may be obtained by dividing Equation (23) by the energy per photon, $h\nu$,

$$\mathcal{N}.d\lambda = \frac{2\pi c}{\lambda^4(e^{hc/\lambda kT}-1)}d\lambda \qquad (24)$$

The Planck Radiation Law indicates (Figure 4) that the spectrum of radiation shifts towards shorter wavelengths as the temperature of the radiator increases. This is a common observation with practical sources. A metal, when heated, radiates first at very long wavelengths in the infrared. As it becomes hotter, it begins to radiate more at shorter wavelengths, first in the red end of the visible spectrum and finally more and more towards the blue. Thus the metal appears successively deep red, red, orange, yellow, and finally white.

The wavelength of maximum emission may be found as a function of the temperature if we take the derivative of the energy density and set it equal to zero. If Equation (21) is expressed in terms of wavelength, we have;

$$U_\lambda.d\lambda = \frac{8\pi}{\lambda^5}.\frac{hc}{e^{hc/\lambda kT}-1}d\lambda \qquad (25)$$

Then, $$\frac{\partial U_\lambda}{\partial \lambda} = \frac{40\pi ch}{\lambda_m^6(e^{hc/\lambda_m kT}-1)} + \frac{8\pi ch}{\lambda_m^5}.\frac{ch}{\lambda_m^2 kT}.\frac{e^{hc/\lambda_m kT}}{(e^{hc/\lambda_m kT}-1)^2} = 0$$

Simplification of this relation gives:

$$\left(1-\frac{hc}{5\lambda_m kT}\right)e^{hc/\lambda_m kT} = 1$$

Replacing $hc/\lambda_m kT$ by x we have:

$$\left(1-\frac{x}{5}\right)e^{x} = 1$$

The solution of the above equation may be obtained by using iterative methods to find $x = 4.965$, thus

$$\frac{hc}{\lambda_m kT} = 4.965$$

or in units of μ and ^{o}K, we will have,

$$\lambda_m T = 2893\ \mu^{o}K \qquad (26)$$

Equation (26) is called Wien displacement formula and relates the wavelength of maximum emission to temperature of a black body.(6)

Another fundamental relation is the Stefan-Boltzmann relation for the total radiant emittance of a black body. This is simply the result of integrating the spectral radiant emittance (Equation 23) over all wavelengths extending from zero to infinity. This integral can be shown to yield,(7)

$$\int_0^\infty R_\lambda \cdot d\lambda = \frac{2\pi^5 k^4}{15c^2h^3} T^4 \qquad (27)$$

We define $\frac{2\pi^5 k^4}{15 c^2 h^3} \equiv \sigma = 5.67 \times 10^{-8}$ watts meter^{-2} $(^{\circ}K)^{-4}$ as the Stefan Boltzmann constant, so that Equation (27) becomes:

$$R = \sigma T^4 \qquad (28)$$

Equation (28) gives the total radiation emitted over the entire spectrum, for a black body. For real bodies, this equation must be modified by the factor of emissivity,

$$R = \epsilon \sigma T^4 \qquad (29)$$

In general, the emissivity ϵ is a slowly varying function of temperature, and its values have been determined for some metals that form important sources of infrared radiation. It should be noted that the ϵ in Equation (29) denotes the total emissivity of the body, and it is therefore the integral of the spectral dependence of emissivity, i.e. $\epsilon = \int_0^\infty \epsilon_\lambda \cdot d\lambda$. The dependence of ϵ on wavelength is a unique property of the radiating body and may be obtained experimentally.

The laws of Planck, Wien, and Stefan-Boltzmann, developed above (through Equations 23, 26, 29), are related to the radiation intensity at the surface of an object. However, when the source is viewed by a detector some distance away from it, the radiant intensity received by the detector decreases with distance. If we consider a blackbody point source S and two detectors; D_1 at a distance d from the source and D_2 at a distance 2d from the source, as in Fig. 5, we can write the following:

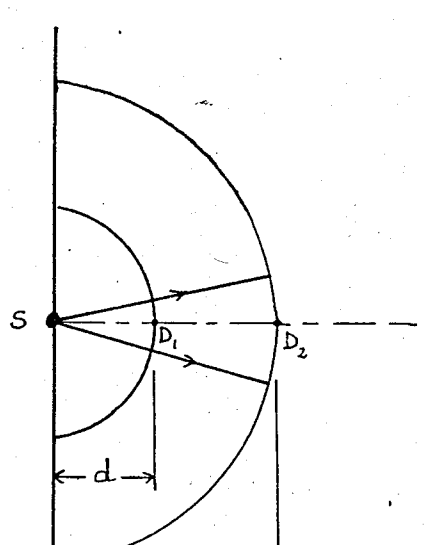

Figure 5: Inverse Square Law

The total radiant emittance from the source as given by Stefan-Boltzmann law, is by definition the radiation power into a hemisphere. The surface area of this hemisphere is $2\pi d^2$ at D_1 and $2\pi(2d)^2 = 8\pi d^2$ at D_2. Therefore, the radiant power received by D_1 is:

$$P_1 = \frac{\text{Emitted Power}}{\text{Receiving area}} = \frac{\sigma T^4}{2\pi d^2} \qquad (30a)$$

Similarly, the radiant power received by D_2 is:

$$P_2 = \frac{\sigma T^4}{8\pi d^2} = \frac{P_1}{4} \qquad (30b)$$

We see that doubling the distance of a detector from a point source quarters the infrared power received by that detector. This result is an illustration of the inverse-square law which states

that the intensity of radiation from a point source varies as the inverse square of the distance from that source.

When the radiating source is a plane extended body, i.e. with finite dimensions, then the position of the line of sight should also be considered in the inverse square law. The effect of angular position is given by Lambert's Law which states that for all wavelength intervals, the radiant intensity varies as the cosine of the angle between the line of sight and the normal to the surface. This is illustrated below:

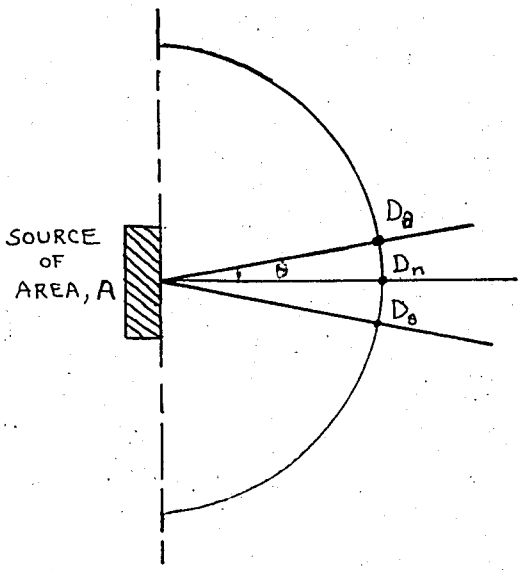

Figure 6: Lambert's Law

The total power received by detector D_n along the normal is given by:

$$P_n = \frac{\sigma T^4 A}{2\pi d^2} \qquad (31a)$$

But the total power received by detector D , θ degrees off the normal will be:

$$P_\theta = \frac{\sigma T^4 A}{2\pi d^2} \cos\theta \qquad (31b)$$

Lambert's law holds for a perfectly diffuse surface, that is, for uniform radiation from all parts of the surface.

B. SOURCES OF RADIATION IN A DETECTION MECHANISM.

In the preceding section, infrared sources were classified according to their emission properties, and it was stated that emission may consist of a line, band, or an entire spectrum of frequencies. The starting point in infrared detection is to determine the strength and spectral content of radiation emitted by the source. This can be done by means of a spectrometer which separates the radiation into its spectral components and measures the relative intensity in each. However, the emission band of the source to be detected, will in general coincide with a lange number of background radiations from naturally occurring infrared sources. Since any object with a temperature above absolute zero radiates in the infrared, many other sources in addition to the main source exist, and these sources are called natural sources. Fortunately, filtering techniques are available to effectively prevent unwanted radiation from falling on the detection apparatus. In order to device an effective infrared filtering, one has to know the nature of the interfering sources, and in particular the quantitative contribution of these background radiations in the range of wavelengths associated with source emission.

Natural infrared sources are classified into three categories, as terrestrial, atmospheric, and celestial sources.(8) Terrestrial sources occur on the surface of earth, and include trees, bushes, rocks, water, sand, and so on. Spectral characteristics of the radiation emitted depend on the source temperature and characteristics of the surface such as its emissivity and reflectivity. In general, terrestrial sources both emit and reflect infrared energy. If suitable filtering techniques can be found, any terrestrial object at a different absolute temperature than its surroundings can be detected through its emission properties. The general level of background radiation from the terrestrial sources (terrain) may be obtained by assuming it as a gray body with an average emissivity of 0.35. The total radiant emittance from a square meter of terrain at 10°C would be:

$$R = 0.35 \times 5.67 \times 10^{-8} \times (283)^4 = 125 \text{ watts/m}^2$$

According to Wien's Law, the corresponding wavelength of peak radiation would be:

$$\lambda_m = \frac{2893}{283} \cong 10\mu$$

It is seen that the infrared radiation leaving the surface of terrain will be most intense in the far infrared. For an accurate figure on terrain radiation, one has to refer to experimental data for the emissivity of the particular surface under consideration. Both the emissivity and the temperature depends

on the nature of vegetation and will be different for such surfaces as asphalt and concrete. These various surfaces come to different temperatures because each has an emissivity which depends on wavelength. Each surface therefore increases in temperature until it is radiating as much power at long wavelengths as it is absorbing from the sun at relatively short wavelengths. However, in a given wavelength range the rates of emission will be different and infrared systems may thus distinguish such features as trees and roads in mapping the terrain.

Atmospheric Infrared Sources: These consist of the gas molecules, water droplets, and dust particles present in the earth's atmosphere. Such constituents do not yield strong emission in the infrared, but they scatter, transmit, and reflect primary radiation illuminating them from both celestial and terrestrial sources. The most pronounced effect of atmospheric constituents is the reflection and scattering of sunlight by day and moonlight by night. Though the solar emission is most intense in the visible region, its effects extend well into the near infrared. Clouds are responsible for most of the reflection of radiation emanating from the sun and the earth. The lower surface of a cloud has radiating characteristics typical of a body at $0^{o}C$, whereas the upper surface radiates as though it were a black body at $-40^{o}C$. Even though the radiance of cloud surfaces is low, the total power radiated may be large due to their great sizes. For wavelengths above 3μ, the total power from the sky background is about 0.85 mW/m^2 of earth's surface. Figure 7 below shows the spectral distribution of radiation reflected from the clouds:(9)

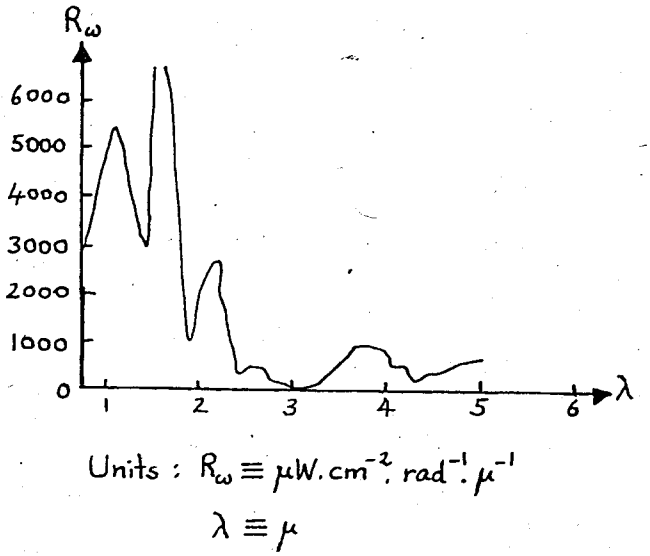

Figure 7: Sky Background

Celestial Sources: The third natural radiation source comprises the celestial bodies, that is the sun, moon, stars, etc. The sun closely resembles a black body source at 6000°K, which is approximately the average temperature of its outer surface. The corresponding wavelength of peak radiation would be 0.5μ .

As viewed from the earth, however, the solar spectrum will not follow a black body distribution since the atmosphere leads to considerable scattering and absorbtion. The relative distribution of solar radiation is shown in Figure 8 as viewed from above the atmosphere and also from the earth:(10)

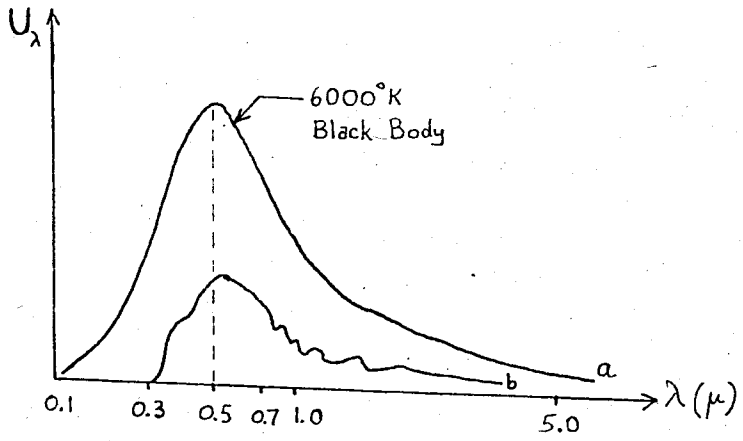

Figure:8

Curve a: Solar spectrum above atmosphere (Relative Scale)

Curve b: Solar spectrum at surface of earth (Relative Scale)

The total radiant power received from the sun is about 89 watts/m^2 normal to earth's surface. The portion of this radiation belonging to wavelengths longer than 3μ is approximately 2 watts/m^2. In the same spectral region, the total power from the sky background radiation amounts to only 0.85 milliwatts/m^2 of earth's surface. We therefore see that, even though the infrared region claims a relatively small portion of the solar spectrum, the sun is still an extremely intense infrared source in comparison to the sky background.

The next important celestial source of infrared is the moon. The bulk of the energy received from the moon is solar radiation reflected from the lunar surface. It is known that the lunar atmosphere contains very small amounts of inert gases, so that the

absorbtion is very slight. Apart from functioning as a reflector, the moon generates its own infrared radiation since lunar temperatures exceed the limit of absolute zero. It has been estimated that the surface dust layer on the moon may reach 373°K during the lunar day and falls to about 120°K during the lunar night. The surface temperature below the dust layer is a constant 230°K, corresponding to a peak radiation at 12.6 μ.

The preceding discussion indicates that the main sources of background radiation are: 1) scattered and reflected solar radiation, 2) atmospheric emissions, and 3) terrestrial emissions. The intensity and spectral distribution of this background varies with the following factors:

1. Water vapor and carbon dioxide contents of the atmosphere
2. Length of path traversed through the atmosphere
3. Temperature of the atmosphere
4. Altitude of the detector above the earth's surface
5. Clouds and haze.

On a relative scale, the spectral distribution of background radiation from the sky is shown in Fig. 9 below:(11)

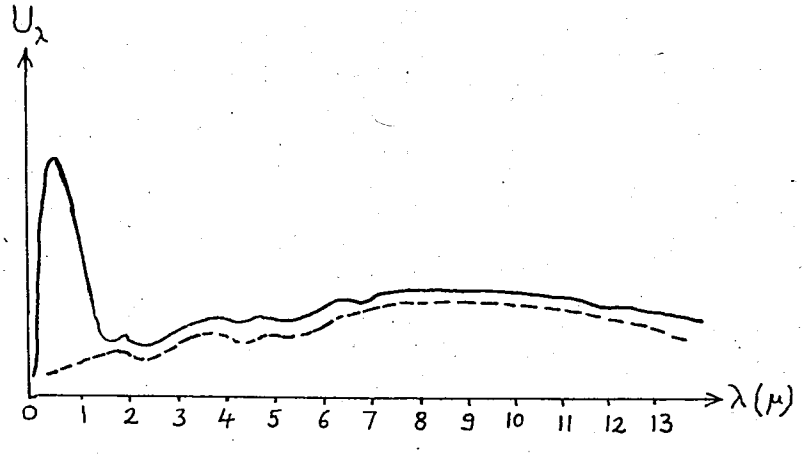

Figure 9: Background Radiation

The effect of scattered and reflected solar radiation is pronounced up to about 3μ. Beyond this limit, the background radiation essentailly consists of emissions from atmospheric constituents such as water vapor, carbon dioxide, ozone, and hydroxyl radicals at their ambient temperatures. At night, that is during the absence of sunlight, the background effect is due to black body radiation from the atmosphere. The effects of daylight background may be greatly reduced by filtering out all radiation below 3μ. In practice, most targets to be detected radiate in a wavelength region beyond 3μ, so that this filtering will help to improve the response of the detector. If the range of operation of the detection system is displaced towards the middle and far infrared wavelengths, however, the background radiation due to the terrain will become more and more pronounced, as indicated before. As a result, the use of band-pass filters will often be necessary, in order that a specified wavelength interval will be permitted to enter the detector. Pronounced

background effects will then correspond to wavelength regions below and above this specified interval.

The properties of filter materials will be discussed later, in connection with infrared transmission phenomena.

Apart from the natural infrared sources discussed so far, various laboratory sources are available for system analysis. Black body characteristics may be very nearly approached by practical cavity radiators made in the form of hallow cylinders or cones. Since high emissivities are desired, the opening provided on the cavity wall should be very small. With a small opening and a perfectly opaque cavity wall, the incident radiation through the opening has an increased probability of being totally absorbed after a series of reflections from the walls. The shape and size of the opening is a problem of choosing for optimum results, because a small opening yields high emissivity but low output, whereas a large opening yields low emissivity but high radiant emittance.(12) The effective emissivity of the cavity radiator will depend on the emissivity of the wall material and the ratio of the aperture area to that of the cavity surface area. In practice, the cavity material is usually a metal or ceramic (e.g., Al_2O_3) blackened to improve absorbtion. A practical cavity radiator used for testing detectors is shown in Figure 10 below:(13)

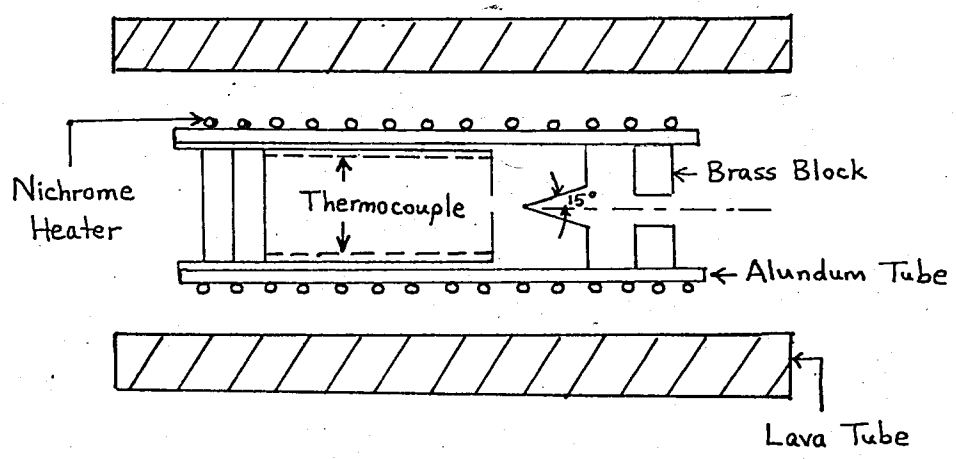

Figure 10: Blackbody Radiator

This laboratory source consists of a conical cavity of 30° vertex angle machined in a copper cylinder. Joulean heating is supplied to a noninductively wound nichrome element wrapped on the outside of the cylinder. Both heater and copper are placed in an insulating lava tube so that the end of the cylinder containing the cavity may be viewed through a small aperture.

When strictly blackbody characteristics are not needed, other artificial sources may be used. In infrared spectrometers a convenient source of radiation is a rod of sintered silicon-carbide (globar) heated by an electric current through it. This device has an average emissivity of 0.78 up to 15μ of wavelength; a maximum emissivity of 0.85 being observed around 9μ. The globar oxidizes and disintegrates at temperatures above 1300°K.

Another common laboratory source is the Nernst glower made of a mixture of Zirconium and Yttrium oxides and heated by means of an

electric current. It can operate at 1800°K in air but has a low mechanical strength.

During recent years, non-thermal sources of infrared radiation have been developed. These include various types of lasers. On the extremely far end of the infrared 600-800 μ region, microwave oscillators such as klystron and magnetron are used to generate infrared radiation.

III. PROPERTIES OF INFRARED TRANSMISSION MEDIA

The necessity of filtering arrangement against background radiations was emphasized in the preceding discussion. In addition to filters, infrared detection systems employ other optical means to improve detector response. Among these are infrared windows and lenses to focus the incoming radiation of desired wavelengths on to the sensing element. Such arrangements give rise to an optical gain and thereby considerably improve the sensitivity of the detector. A knowledge of the infrared transmission properties of different media is therefore necessary for the design of an arrangement with maximum optical gain. In this section, we will discuss the properties of important infrared optical materials and indicate their applications as filter, lens, or window materials.

A. ATMOSPHERIC TRANSMISSION.

Transmission of infrared radiation through the earth's atmosphere is dependent upon the concentration and distribution of gaseous and molecular particles composing the atmosphere. The concentration of such particles in turn depends on meteorological conditions, particularly in the lower atmosphere where the water vapor, gaseous and dust contents may vary continuously. Atmospheric transmission is therefore a function of altitude above sea level and the weather conditions.

The earth's atmospheric gases consist of polyatomic molecules such as methane (CH_4), triatomic molecules such as water vapor (H_2O), nitrous oxide (N_2O), carbon dioxide (CO_2), ozone (O_3), and diatomic molecules such as carbon monoxide (CO). At low altitudes from the earth, the temperature is not high enough to cause the dislocation of these molecules into their individual atoms as in the case of solar atmosphere. As a result, the earth's atmosphere exhibits the characteristics of band spectra rather than line spectra which is produced only by monatomic gases.

Attenuation of radiation throughout the infrared region is dominated by two processes: 1) resonance absorbtion, 2) scattering. The phenomena of resonance absorbtion may be explained as follows: the periodic motions of electrons in the atoms of a source, vibrating and rotating at certain frequencies, result in the radiation of electromagnetic waves at those frequencies. Similarly, atmospheric constituents contain bound charges or electrons with characteristic frequencies depending on the molecular structure. When the electric field vector of an incident electromagnetic wave varies with a frequency which coincides with the natural vibration frequency of a charged particle in the atmosphere, a large amplitude of vibration results. The energy is absorbed and reradiated as resonance radiation of the same frequency. The resonance radiation is uniformly distributed in all directions, so that in a particular direction, the incident radiation is in effect attenuated.

The second process which attenuates the incoming radiation is, scattering by dust nuclei and water droplets in the atmosphere. The form of attenuation is negligible in the middle infrared,

region at wavelengths longer than 4μ, but increases rapidly for shorter wavelengths. Absorbtion may be much greater than scattering or vice versa, depending upon the nature of the atmosphere, the particle size, and wavelength; but both phenomena are usually present. For a given wavelength, it has been found that the radiant intensity decays exponentially through a path of the atmosphere, thus:

$$E = E_o e^{-(\alpha+K)x} \qquad (32)$$

where E_o = intensity of incident infrared radiation
E = intensity of emergent infrared radiation
α = absorbtivity
K = scattering coefficient
x = path length in the atmosphere.

The sum of factors α and K is usually called the extinction coefficient of the medium.[14] The value of absorbtivity depends on the wavelength under consideration. The scattering coefficient is a function of the scattering particle size which is random throughout the atmosphere. If particle sizes are larger than the constituent molecules in the atmosphere, the scattering coefficient becomes independent of wavelength.

Among atmospheric constituents, water vapor and carbon dioxide are the most important absorbing molecules over a range of altitudes extending from sea level to 15000 m. The concentration of H_2O by volume varies between 0.001% and 1% depending upon altitude and meteorological conditions.

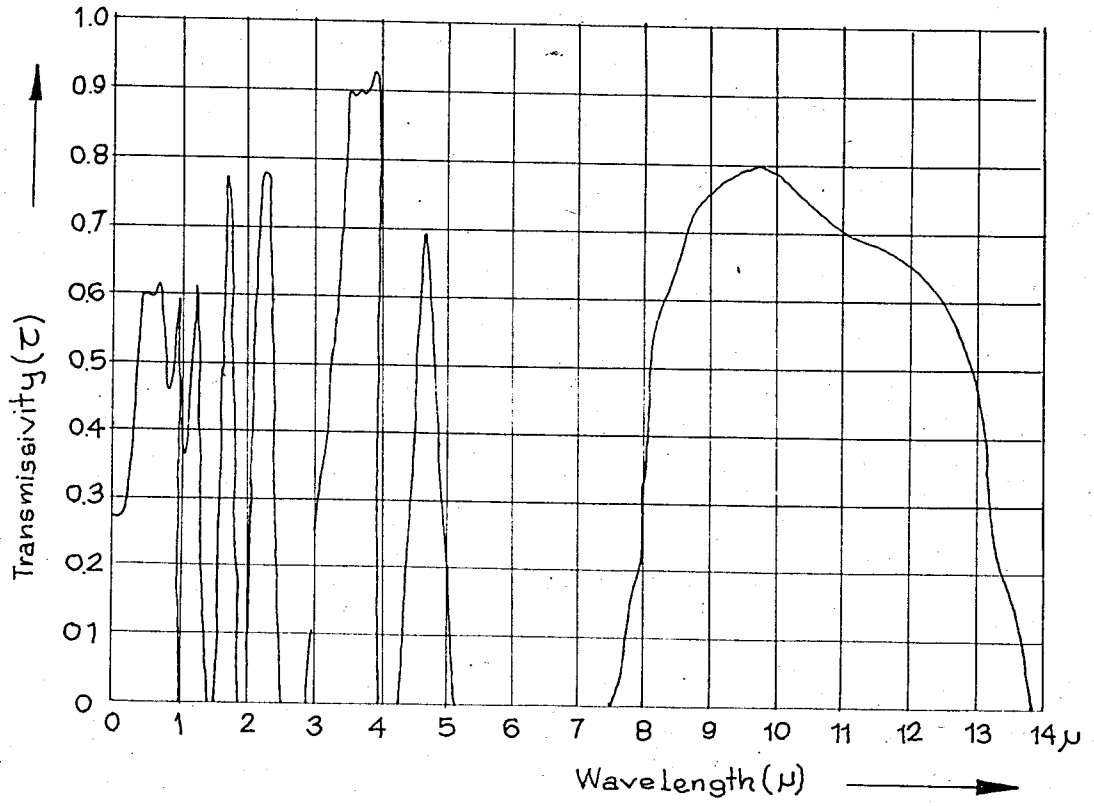

Fig. 11
Atmospheric transmission[15]

Carbon dioxide concentration is almost constant at 0.03% by volume although larger concentrations are encountered in an air mass which has been over heavy vegetation. The absorbtion characteristics of ozone become significant only at high altitudes; the concentration of ozone being 0.001% by volume at an altitude of 35000 m.

The transmission characteristics of the atmosphere as a whole are depicted in Figure 11 for wavelengths up to 14 μ.

B. TRANSMISSION THROUGH SOLIDS.

Apart from the atmosphere, which is a natural medium encountered in detection systems, the transmission properties of solid media are the most important for design considerations.

Several mechanisms account for the transmission characteristics of solid materials. The most important of these mechanisms include 1) fundamental absorbtion, 2) characteristic absorbtion, 3) free-carrier absorbtion, 4) intrinsic and extrinsic absorbtion (for semiconductors). The mechanism of fundamental absorbtion refers to the interaction of electromagnetic waves with the lattice of the solid, and is therefore also called lattice absorbtion. Characteristic absorbtion is due to molecular vibrations and rotations in the solid, and results in the attenuation of those incident frequencies identical with the characteristic vibrational frequencies of the molecules. Free carrier absorbtion refers to the interactions between free electrons in the solid and the incoming radiation. This mechanism is important in metals since free electron densities are largest for metals. The last mechanism, intrinsic and extrinsic absorbtion, is generally applicable to semiconductors. It causes the excitation of electrons across the forbidden energy levels (the energy gap) into the conduction band of the semiconductor, and also transitions from various impurity energy levels and the conduction or valence band.

Included in the broad category of solid optical materials are dielectrics, glasses, plastics, metals, and semiconductors. The

infrared transmission properties of these solids are different for each type, and a general discussion will be given in the following paragraphs. Optical, mechanical, and chemical properties of important infrared materials are given in Table I.

1. Dielectrics: Dielectrics typically possess good transmission in certain infrared regions and are suitable for use as windows, filters, and lenses. Their reflectivity is low in comparison to other types of solids. Their thermal and electrical conductivities are low, and they are frequently brittle. For single crystal dielectrics, fundamental absorbtion accounts for most of the experimentally measured attenuation. Characteristic absorbtion is limited to visible, ultraviolet and x-ray regions of the spectrum. At room temperature, the number of free electrons in a dielectric is so small that free carrier absorbtion is also insignificant. In polycrystalline dielectrics, scattering may cause attenuation of the incident radiation. This effect is due to the change in index of refraction at the boundaries between individual crystals. Most dielectrics transmit in the visible but tend to absorb in certain infrared regions.

2. Glasses: In general, optical glasses are suitable for wavelengths shorter than about 2.8μ. The transmissivity of common glasses abrubtly drops to very small values after this wavelength limit. Two special glasses may be employed for longer wavelengths: A high silica glass under the trade name Vycor transmits up to 3.3μ, and fused silica can be used in applications requiring response up to 4.5μ. During recent years, special types of glasses containing germanium dioxide, lead tellurate, and various barium-

titanium compounds in addition to common silicates, have been developed, but these samples are not stable and tend to darken and discolor with age.(16) Glasses may be employed as window materials at high temperatures since their transmission is not strongly temperature dependent. They offer an economical choice as an optical material for the near-infrared detectors.

3. Plastics: Plastics are composed of chains of molecular groups which cause characteristic absorbtion. The number of such groups is so large that infrared transmission is limited to a number of narrow wavelength intervals. If the transmission band of the plastic material coincides with the band to be detected, the sample may be used as a window material or as a filter. Only thin samples of plastics exhibit good transmission in a given narrow band of wavelengths. In practical systems, this property is undesirable since a thin plastic specimen is not suitable for applications requiring ruggedness, strength, and resistance to temperature variations.

A representative plastic material is plexiglass which offers almost full transmission in the visible and near-infrared frequencies, but a strong absorbtion band centered at about 3.3 limits its use in most practical systems. Other plastic materials have not found any use in infrared optics.(17)

4. Metals: Metals are characterized by the fact that both their absorbtivity and reflectivity are large. A large part of the optical absorbtion in metals is free carrier absorbtion since the concentration of free electrons is very high. As a result, metals appear opaque in the infrared. They can be used for shielding

various parts of the detection system against radiation. To give an example, copper has an average reflectivity of 0.90 in the near infrared. This value increases with wavelength and for thin films of metals, the reflectivity is even higher.

5. Semiconductors: In contrast to dielectrics, semiconductor materials are opaque in the visible but transparent in a large part of the infrared. This behavior may be explained in terms of the energy band structure of semiconductors. Since the energy of a quanta is inversely proportional to wavelength, electromagnetic radiation of sufficiently short wavelengths will induce transitions across the energy gap of a semiconductor. The longest wavelength (λ_o) that can cause intrinsic absorbtion and activate electrons into the conduction band, will be:

$$\lambda_o = \frac{hc}{E_g} \qquad (33)$$

where (E_g) is the forbidden gap energy. If the values of E_g are substituted in Equation (33), it is found that λ_o falls near the visible region. Thus the semiconductor will cut off all radiation up to the infrared, by a mechanism of intrinsic absorbtion. The value of λ_o is $1.10\,\mu$ for silicon and smaller for complex semiconductor materials.

In addition to their filtering action in the visible region of the spectrum, semiconductors may be used as infrared lenses since their indices of refraction are high.

A consideration of the optical, thermal, and mechanical properties of various important materials, as listed in Table I, will in general be sufficient for the choice of a material as a lens, window, or filtering element in an infrared detection system.

TABLE I :

Material	Description	Wavelength limits, μ	Index of refraction	Cold-water solubility g/100g H_2O	Melting point, °C	Young's modulus 10^6 psi	Knoop hardness	Density g/cm³	Coeff. of thermal expansion 10^6/°C	Maximum size, D	Relative cost
Artificial sapphire	Hexagonal crystal; hard to scratch; no cleavage; excellent mechanical strength (see Table 6-2)	0.17–5.3	1.77 at 1.0μ	0.8×10^{-4}	2030	53	1,370	3.98	6.7 (parallel) 5.0 (perp.)	4½ in. diam	high
Fused quartz (SiO_2)	Isotropic; good mechanical properties	0.2–4.0	1.45 at 1.0μ	10	1700	10^{-1}	470	2.21	0.5	limited by practical optical homogeneity	moderate
Silicon	Steel-gray cubic crystal; transmission decreases above 300°C; soluble in HF, HNO_3 (see Table 6-2)	1.2–15	3.4 at 10μ	0	1420	1.9×10^{12} dyne/cm²	1,150	2.33	4.2	approx. 7 in. diam.	high
KRS-5 (TlBr-TlI)	Red cubic crystal; toxic; no cleavage; difficult to polish; scratches easily; strains easily	0.6–38	2.37 at 10μ	0.05	415	2.3	40	7.37	58	approx. 5 in. diam.	high
KRS-6 (TlBr-TlCl)	Colorless cubic crystal; toxic	0.4–30	2.18 at 10μ	0.32	424	3.0	35	7.2	51	approx. 7.5 in. diam.	high
Cesium bromide (CsBr)	Colorless cubic crystal; Hygroscopic; Soft; soluble in alcohol	0.2–40	1.66 at 10μ	124	630	2.3		4.5	48	approx. 2 in. diam.	moderate
Potassium bromide (KBr)	Colorless cubic crystal; soft; hygroscopic; cleaves	0.2–32	1.53 at 10μ	66	728	3.0	6	2.75	41	approx. 7½ in. diam.	moderate
Periclase (MgO)	Hard isotropic crystal; cleaves (see Table 6-2)	0.25–7	1.71 at 2.0μ	1.2×10^{-4}	2800	36	690	3.59	18	approx. 3 in. diam.	high
Rutile (TiO_2)	(see Table 6-2)	0.4–5.2	2.6 at 1.0μ	0	1830		880	4.25	9 parallel 7 perp.		
Potassium chloride (KCl)	Colorless cubic crystal; soft; hygroscopic; cleaves; soluble in glycerin, ether, alkali	0.21–25	1.46 at 10μ	35.5	768	4.3	8	1.99	36	approx. 7½ in. diam.	moderate
Potassium iodide (KI)	Colorless cubic crystal; cleaves; very soft; very hygroscopic; soluble in alcohol, ammonia	0.2–31	1.67 at 10μ	127						approx. 7½ in. diam.	moderate
Cesium iodide	Cubic crystal; soft; hygroscopic; cleaves	0.24–52	1.74 at 10μ	44	621	0.8		4.53	50		
Lithium fluoride (LiF)	Colorless cubic crystal; soft; cleaves; soluble in acid	0.12–7	1.38 at 2.0μ	0.26	870	11	110	2.6	36	approx. 5 in. diam.	moderate
Calcium fluoride (CaF_2)	Colorless cubic crystal; easily scratched; cleaves; soluble in ammonium salts	0.13–9.5	1.42 at 2.0μ	1.5×10^{-4}	1400	15	158	3.18	23	approx. 6 in. diam.	moderate
Lead fluoride (PbF_2)		0.25–12	1.75 at 1.0μ		822						
Barium fluoride (BaF_2)		0.15–13	1.6 at 12μ	0.16	1280	8	82	4.9			
Germanium		1.8–15+	4.1 at 10μ		942	15		5.33	6.1		
Spinel ($MgO \cdot Al_2O_3$)		0.3–5	1.73 at 1.0μ	0	2050		1,140	3.62	6		

IV. DETECTION METHODS

The infrared detector is a transducer where the energy of incoming electromagnetic radiation is changed into an electrical signal. Detection process is based on measuring the change in some physical property of the sensing element as a result of interaction with radiation. Depending on the nature of the physical phenomena employed in detection, infrared detectors are broadly classified into two types: thermal detectors and photon detectors.

Thermal detectors make use of the heating effect of radiation. The temperature increment induced on the sensing element is detected by measuring the changes in some property of the element which depends on temperature. Usually, this property is the resistance of the material.

In photon detectors, radiation is converted into an electrical signal directly, rather than through some temperature dependent process. The detection phenomena employed in photon detectors is the release or transfer of charge carriers in the material, as a result of interaction with absorbed quanta. Since large quanta energies correspond to short wavelengths ($E = hc/\lambda$), only radiation of sufficiently short wavelengths will be effective in creating the physical phenomena utilized. Consequently, photon detectors will not respond after a well defined wavelength cutoff. Furthermore, the response of a photon detector at a given wavelength will be proportional to the rate at which photons of that wavelength are

absorbed. In practice, the output signal of a photon detector is governed by a "quantum efficiency." Since every incident photon will not be effective in causing the release or transfer of a charge carrier, the efficiency is not constant but depends on the wavelength, the detector response will no longer be linear, as observed with practical detectors.

In contrast to photon detectors, thermal devices are not selective to wavelength and respond to radiation of all wavelengths. This follows from the fact that thermal detectors measure the rate at which energy is absorbed, rather than the rate at which quanta are absorbed. In practice, due to material imperfections, the exposed surface may have a low absorbtivity in a given spectral interval, so that the energy in the corresponding interval is not utilized effectively. For such cases, the response of a thermal detector may become selective at certain wavelength bands.

A number of different physical phenomena are employed in the design of detectors. These phenomena are termed as photon effects and thermal effects. In the remaining part of this section, important effects will be discussed so that any limitations in a given mode of operation become clearly established.

A. PHOTOEMISSIVE EFFECT.

If radiation of wavelength less than a critical value falls upon the surface of certain materials, it is found that electrons are emitted from the surface. The relationship between the energy of the emitted electron and the properties of the surface may be expressed as:

$$\frac{1}{2}mv^2 = \frac{hc}{\lambda} - e\phi \qquad (34)$$

where $(e\phi)$ is the work function of the material under question. The significance of the work function is that it represents the minimum energy of quanta necessary to initiate photoemission. The longest wavelength λ_o that will produce photoemission is found by setting Equation (34) equal to zero, thus,

$$e\phi = \frac{hc}{\lambda} \qquad (35)$$

If the work function is expressed in electron volts and the wavelength in microns, the critical wavelength becomes,

$$\lambda_o = \frac{1.24}{e\phi} \qquad (36)$$

Equation (36) states that the sensitive element in a photoemissive detector must have a low work function in order to yield an output signal at long wavelengths of incident radiation. Among the elements in periodic table, cesium has the lowest work function of 1.9 eV, so that a photocathode made of cesium would respond to wavelengths up to 0.65μ. Since this limit lies in the visible region, it is seen that none of the elements could by itself serve as a photoemitter with an infrared response.

It has been possible to manufacture multielement photoemissive surfaces with responses in the near infrared. The most common one is the Silver-Oxygen-Cesium surface with a work function of 0.98 eV.

The corresponding wavelength limit is about 1.2 μ.

The photoemissive process is extremely fast, the time constants being in the order of 10^{-8} sec for common surfaces. However, due to the very limited response of photoemissive process in the infrared, detectors built on this effect have not found much practical use.

B. PHOTOCONDUCTIVE EFFECT.

Photoconductivity is observed in insulators and semiconductors exposed to radiation of sufficiently short wavelengths to promote carrier generation. For insulators, free carrier concentration is zero at room temperature and in the absence of radiation. If sufficient quantum energy is applied, the electrons in the valence band of the insulator may be excited across the energy gap into the conduction band. In such a case the insulator becomes conductive, and a measurement of its conductivity will indicate the content of incident radiation.

Semiconductors, however, contain free electrons and holes at any temperature. As a result, their conductivity is not zero in the absence of radiation. When radiation falls on a sample of semiconductor, two type of excitations cause an increase of conductivity. The first is intrinsic excitation in which hole-electron pairs are generated by a transfer of electrons from valence band to the conduction band. The condition for this process to occur, may be written as,

$$\frac{hc}{\lambda} \geq e E_g \qquad (37)$$

where Eg is the energy gap expressed in electron volts.

If the semiconductor contains donor or acceptor impurities, a second type of action, extrinsic excitation takes place. This consists of a transfer of electrons from valence band into acceptor levels or from donor levels into the conduction band. It is possible to introduce a controlled amount of impurity atoms into a semiconductor and thus make use of the extrinsic excitation phenomena for detection. Since donor and acceptor levels are located near conduction band and valence band edges respectively, the necessary energy to cause extrinsic excitation is less than that represented by Expression (37). As a result, radiation of relatively long wavelengths may be sufficient to cause extrinsic activation. Impurity type of photoconductive detectors therefore have a response in longer infrared wavelengths.

In order to evaluate certain criteria to be used in the selection of photoconductive sensors, an analysis of intrinsic photoconduction is given below.

The conductivity (σ_o) of the sensor in the absence of radiation may be written as:

$$\sigma_o = \frac{e}{AL}\left(n_o\mu_n + p_o\mu_p\right) \qquad (38)$$

In the above expression, (A) is the cross section of the sample, (L) is its length, (n_o) and (p_o) are the total number of electrons and holes and (μ_n, μ_p) are the respective mobilities and (e) is electronic charge in coulombs. If (P) watts of radiant power fall on the

sensor, the number of hole-electron pairs produced per second (Q) is given by:

$$Q = \eta \frac{P}{h\nu} \tag{39}$$

where (η) denotes the "quantum efficiency", or the number of hole-electron pairs generated for each incident photon. Taking an average lifetime of (τ_n) for additional electrons and (τ_p) for additional holes, the total number of carriers are increased by:(19)

$$\Delta n = Q\tau_n$$
$$\Delta p = Q\tau_p \tag{40}$$

The change in conductivity of the sensor may be written by analogy to Equation (38); thus:

$$\Delta\sigma = \frac{e}{AL}\left(\Delta n.\mu_n + \Delta p.\mu_p\right) \tag{41}$$

If Equations (40) are substituted above, we have,

$$\Delta\sigma = \frac{eQ}{AL}\left(\mu_n\tau_n + \mu_p\tau_p\right) \tag{42}$$

The corresponding increment in the <u>conductance</u> of the sensor would by definition be given as:

$$\Delta g = \Delta\sigma.\frac{A}{L} = \frac{eQ}{L^2}\left(\mu_n\tau_n + \mu_p\tau_p\right) \tag{43}$$

Under an applied voltage, the current induced by the incident radiant power becomes:

$$\Delta I = V.\Delta g = \frac{eQ}{L^2}(\mu_n \tau_n + \mu_p \tau_p)V \qquad (44)$$

For a sensitive detector, the expression given by (44) should be large. This means that the detector material should possess large mobilities and large carrier lifetimes. Furthermore, the length of the sensing element should be small.

In practice, it has been found that Silicon and Germanium samples doped by gold or mercury, possess the above requirements. Other compounds commonly employed, are lead sulfide (PbS), lead selenide (PbSe), lead telluride (PbTe), strontium sulfide (SrS), and indium antimonide (InSb).

The change in conductivity of a photoconductive detector exposed to radiation may be detected by means of the circuit shown in Figure 12 below.

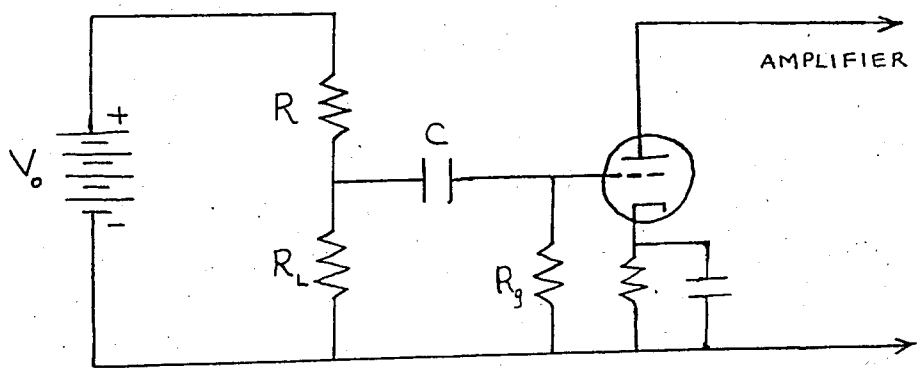

Figure 12: Detector Circuit

The photoconductor of dark resistance R is placed in series with a load resistor R_L and a battery of emf V_o. Infrared radiation falling on the detector is modulated or chopped so as to give a time-varying output suitable for amplification. Absorbtion of radiation causes a decrease in the resistance of the sensing element, and as a result the circuit current increases. This current increment causes a greater fraction of V_o to appear across the load resistance, R_L. The voltage across R is impressed into the grid circuit of the first amplification stage. In Fig. 12, R_g represents the bias resistor of the tube, whereas the capacitor C serves to prevent any d.c current from entering the grid.

In the absence of radiation, the voltage V appearing across the load is given by:

$$V_L = V_o \frac{R_L}{R + R_L} \qquad (45)$$

The effect on V_L due fo: a change in the resistance of the sensing element may be obtained by differentiating Equation (45) with respect to R. We get:

$$\Delta V_L = -V_o \frac{\Delta R . R_L}{(R + R_L)^2} \qquad (46)$$

It is seen from Equation (46) that the signal may be maximized if we let $R = R_L$. Under this matching condition, the signal output from the sensor, or the amplifier input may be written as:

$$\Delta V_L = -\frac{V_o . \Delta R}{4R} \qquad (47)$$

C. PHOTOVOLTAIC EFFECT.

Electromagnetic radiation falling on a p-n junction will induce a voltage which may be measured directly from the ohmic contacts, without a need for a bias battery or a load resistor. This is called the photovoltaic effect, and it is illustrated in Fig. 13 below. In the absence of radiation falling on the junction, the Fermi Levels in the p and n regions are aligned. An internal electric field $\vec{\mathcal{E}}$ exists at the

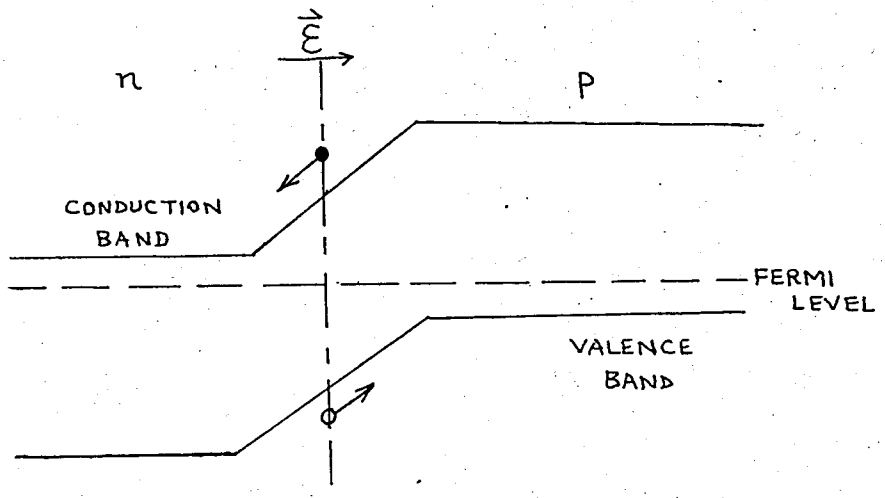

Figure 13: Photovoltaic Effect

barrier. A photon of sufficiently short wavelength will produce a free electron-hole pair when absorbed at the barrier. The action of the electric field at the barrier separates the pair, moving the electron into the n-type material and the hole into the p-type material. Since excess electrons have moved into the n-type region and excess holes into the p-type region, the n-type region is

charged negatively, and the p-type region is charged positively. As long as radiation falls on the junction, electron-hole pairs will be formed and separated by the internal field at the junction. If the semiconductor ends are short circuited by an external conductor, a current will flow in the circuit as long as radiation falls on the junction. If the ends are open-circuited by a high impedance voltmeter, a voltage will exist as long as radiation falls on the sample.

It is to be noted that radiation falling on points remote from the junction will not contribute to the photovoltaic effect. If carriers are generated at a distance from the junction equal to the diffusion length of electrons or holes, those carriers that survive recombination, may reach the junction and contribute to the effect.(20)

Although a voltage appears across the open ends of the p-n junction without need for a bias, the junction may also be operated under external reverse bias. In this case the junction constitutes a photodiode, and detection is based on measuring the change in reverse saturation current as a result of absorbed radiation. The argument may be illustrated by considering the current-voltage characteristics of a p-n junction diode:

$$I = I_s\left(1 - e^{\frac{eV}{kT}}\right) \qquad (48)$$

In this expression, I_s is the reverse saturation current in the absence of radiation and V is the external bias. If radiation

falls on the junction, the current will be increased by an amount ΔI so that:

$$I = \Delta I + I_s \left(1 - e^{\frac{eV}{kT}}\right) \qquad (49)$$

For a large reverse bias ($V<0$), the exponential term is negligibly small so that:

$$I \cong \Delta I + I_s \qquad (50)$$

Thus, by connecting ends of a reverse biased p-n junction to a sensitive ammeter, it is possible to read the amount of current generated by the incident radiation, as:

$$\Delta I = I - I_s \qquad (51)$$

where I is the ammeter reading and I_s is the reverse saturation current of the diode corresponding to the applied reverse bias. The situation is illustrated in Fig. 14, in which the current-voltage characteristics of the diode are shown in the absence and presence of radiation.

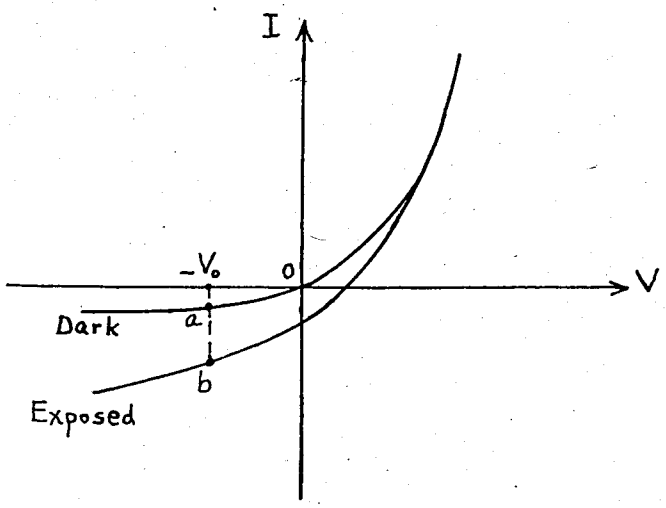

Figure 14: p-n junction characteristics

As shown in Figure 14, the reverse saturation current of the diode is that corresponding to point a on the absence of radiation, and when reverse biased at $-V_0$. The reverse saturation current increases to a value corresponding to point b when radiation is allowed to fall on the diode. The increment ab is the net effect of radiation in terms of diode current. In practice it is desirable to have a very low reverse saturation current in the absence of radiation so that the current increment is large. Photovoltaic phenomenon is not very commonly utilized in infrared detection, but In Sb, In As, Ga As, and Se-SeO have been used as detectors in some near-infrared photovoltaic devices.

D. PHOTOELECTROMAGNETIC EFFECT (P.E.M.).

The PEM effect is basically a diffusion effect in a magnetic field. It is observed in semiconductors immersed in a magnetic field, as shown in Fig. 15:

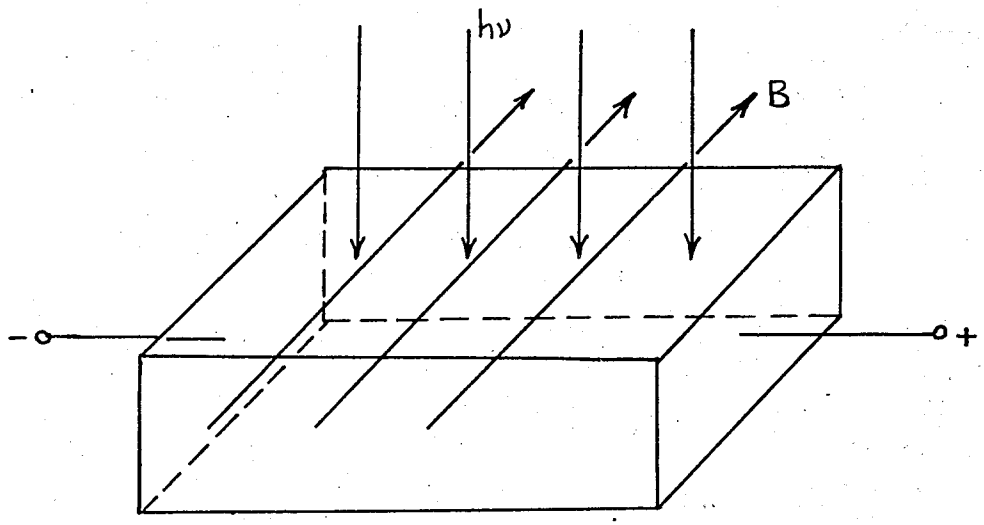

Figure 15: PEM Effect

In Fig. 15, photons of wavelength sufficiently small to liberate hole-electron pairs, are absorbed at the exposed surface of the semiconductor sample. The carriers generated as a result of radiation will diffuse from the surface into the interior. Since they are moving in a transverse magnetic field, the carriers experience a force in a direction normal to the plane of the magnetic field and the Poynting vector and are separated, the holes deflecting toward one end of the sample and the electrons toward the other. If the sample ends are short circuited externally, a current will flow

as long as radiation is absorbed at the front surface. If the sample ends are open circuited, a voltage will appear as long as radiation is absorbed. The photosignal due to the PEM effect is given in terms of either the short circuit current or the open circuit voltage.

In order to obtain good response from a PEM detector, one should reduce surface recombination so that carriers generated there, will diffuse into the bulk before recombination. The sample thickness for optimum response corresponds to the diffusion length for the carriers. PEM detectors have been constructed from InSb and InAs crystals, and in general, they show good response with materials possessing high mobilities and short lifetimes.

E. THERMAL EFFECTS.

The detection phenomena discussed so far have fallen into the category of photon effects in which incident photons below a certain threshold wavelength are absorbed, to give rise to excess charge carriers. Because photon detectors respond to the rate at which photons are absorbed, their spectral responses were seen to be dependent upon the energy of photons, that is the wavelength of radiation.

Another category of detectors, based on thermal effects, will be taken up in full detail in this work. In the following paragraphs, the phenomena of thermal detection will be briefly described. This background, together with the general principles treated so far, will be used to give an account of thermal detection theory and its experimentation.

As stated previously, thermal detectors make use of the heating effect of radiation. Associated with all thermal detectors is some form of thermal mass, the temperature of which changes when it absorbs radiation. From $Q = m.c.\Delta T$ it is apparent that large temperature changes per unit radiant power absorbed, are associated with small thermal masses. As a result, the sensitive elements of most thermal detectors are small. The most well-known forms of thermal detectors are the bolometer and the thermocouple.

1. Bolometer: Bolometers may be of three types: metal, semiconductor, and superconductor. Metal and semiconductor types are operated at ambient temperatures, whereas the superconducting bolometer must be cooled to temperatures near absolute zero.

The resistance of a metal increases linearly with small changes in temperature, thus:

$$R = R_o[1 + \gamma(T - T_o)] \qquad (52)$$

where R_o is the resistance at T_o and R is the resistance corresponding to $T_o + \Delta T$. The value of γ being about 0.005 per °C for many metals and it is almost independent with temperature. It is called the temperature coefficient of resistance.

Semiconductors exhibit a much more pronounced dependence of resistance on temperature, than do metals. Their resistance is generally given by an equation of the form,

$$R = R_0 e^{\frac{\beta}{T}} \qquad (53)$$

where β is a constant characteristic of the semiconductor. As seen from Equation (53), the resistance of a semiconductor decreases with temperature, and due to exponential dependence, the resistance is very sensitive to temperature variations. The temperature coefficient of resistance for most semiconductors is between 0.03 and 0.04 per ^{o}C. This value is seen to be about ten times greater than for a metal and explains why semiconductors should be preferred as bolometer materials.

Semiconductor bolometers are known as thermistor bolometers, thermistor denoting thermally sensitive resistor. There are two common thermistor materials, developed originally by Bell Telephone Laboratories. They consist of the oxides of nickel, cobalt, and manganese, constructed in the form of flakes about 10μ thick. The flakes are mounted on heat dissipating substrates known as thermal sinks. Radiation falling on a flake warms it. If the radiation is removed, the flake returns to its original temperature with a decay time depending on the thermal conductance between the flake and the sink. Fast response is obtained by mounting the thermistor directly on a solid sink.(21)

In measuring circuits, two identical flakes are mounted in the same housing, with a shield over one to prevent signal radiation from falling upon it. The shielded flake serves to compensate for temperature changes in the absence of radiation. Figure 16 shows the bridge circuit arrangement employed in thermistor bolometer detectors.(22)

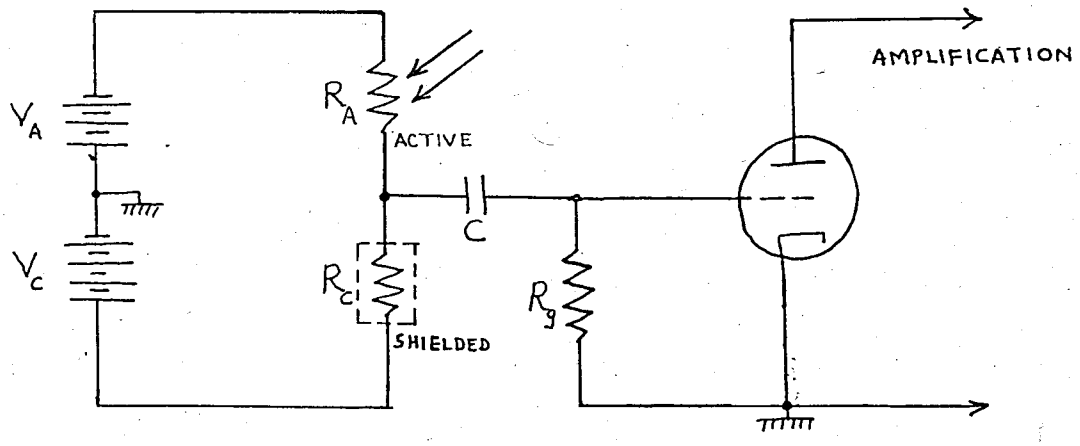

Figure 16: Bolometer Circuit

In the absence of an input radiation, the bridge is balanced since the flakes are identical. Radiation falling on the active flake reduces its resistance, causing the bridge to be unbalanced. This yields an output signal across R_c, to be fed into the first stage of amplification. As with other types of infrared detectors, the input radiation is chopped (modulated) to obtain drift-free amplication.

Superconducting bolometers utilize the sharp change in resistance of some materials (e.g., lead, tin, tantalum, niobium nitride) near the temperature of absolute zero. As the temperature of a superconductor is reduced from room temperature, the resistance decreases linearly for metals. However, as the temperature approaches a critical value T_o, the resistance sharply drops to zero. Below the critical temperature, the material is termed to be superconducting, its resistance being zero. The rapid change in resistance from normal to superconducting state occurs over a small

fraction of a degree. For practical materials, the critical temperature ranges from 1°K to 15°K. If the bolometer element can be maintained at its critical temperature by means of a servo system, considerable resistance increase will be obtained by allowing radiation to fall on the superconductor. The situation is further clarified in the resistance-temperature curve of a superconductor as shwon in Figure (17):

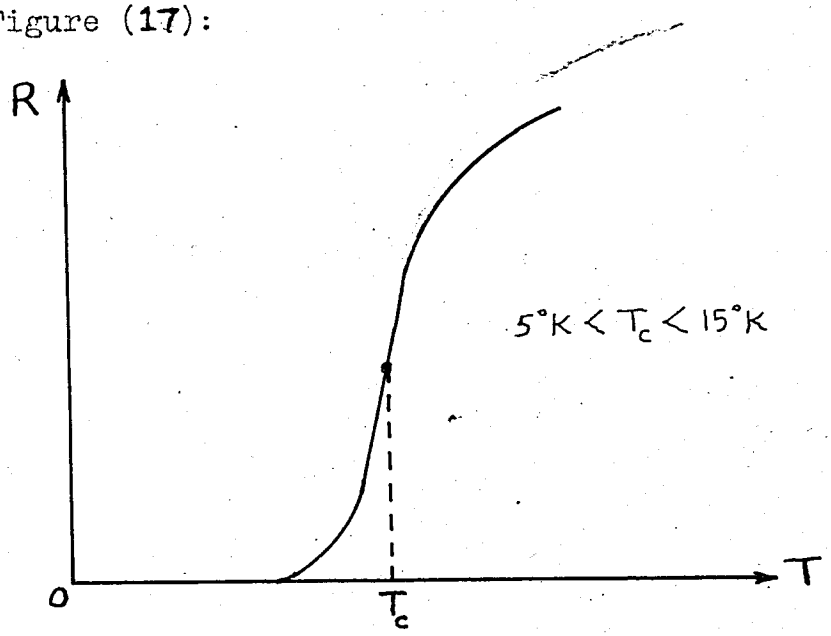

Figure 17: Superconductivity

Superconducting bolometers have not found commercial use due to the difficulty of obtaining and maintaing detector temperature precisely at the critical value of temperature.

2. Thermocouple: The radiation thermocouple is one of the earliest infrared detectors. It consists of a low mass junction mounted on a blackened receiver between two different metals, as shown in Figure (18). The metals are designated A and B. When the receiver absorbs radiation, its temperature is increased by ΔT.

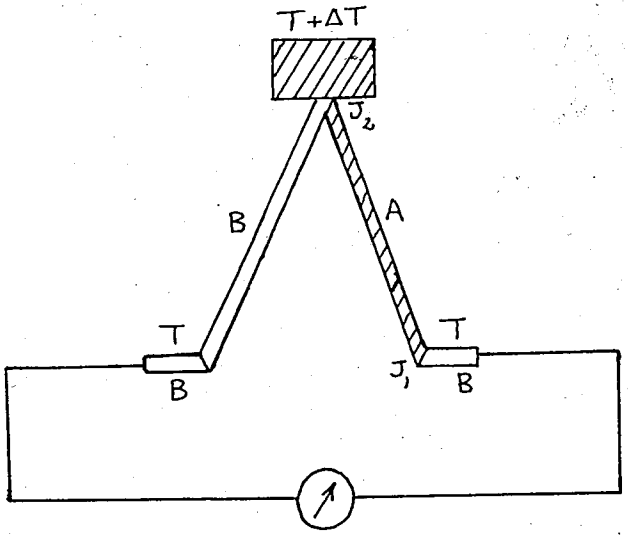

Figure 18: Thermocouple

This temperature difference ΔT between junctions J_1 and J_2 will cause a thermoelectric emf V to be set up between them. The magnitude and direction of V is determined by the thermoelectric properties of substances A and B; and for small temperature variations as encountered in infrared detection, it is given by:

$$V = P_{AB} \cdot \Delta T \qquad (54)$$

where P_{AB} is the "thermoelectric power" between materials A and B.(23) Between Lead and Bismuth, $P_{AB} = -60\,\mu V/^{\circ}C$, between Lead and Antimony, it is + 40 $\mu V/^{\circ}C$.

A widely used form of the thermocouple is the <u>radiation thermopile</u> consisting of a series connection of thermocouple junctions. Since the voltage outputs are added, the thermopile has a larger response for a given temperature interval, but the response time

is increased due to larger masses of active elements. Commercial detectors operating on thermal phenomena have response times near 1.5 msec for thermistor bolometers, and 36 msec for radiation thermocouples.(24) In general, there is no clearly defined cutoff wavelength in the spectral response of thermal detectors.

V. ANALYSIS OF THERMISTOR BOLOMETERS

The infrared system is often designed around the characteristics of the infrared detector. These characteristics are defined by certain figures of merit describing the performance of detectors under specified operating conditions. The important figures of merit universally accepted in infrared technology will be given below. In the subsequent analysis of thermister bolometers, these figures of merit will be evaluated in order to obtain theoretical performance characteristics.

Performance Criteria may be grouped into three categories defining the utility and efficiency of a detector under given conditions.

A. NOISE EQUIVALENT POWER (P_n).

This is the minimum radiant power which would give rise to a signal voltage equal to the noise voltage from the detector. Since the definition implies a signal-to-noise ratio of unity, this figure is a measure of the minimum power that can be detected. Any incident power smaller than P_n will give rise to an output signal that is largely dominated by the noise voltage of the detector. When measuring P_n, the temperature of the black-body radiation source is usually 500°K, the reference bandwidth is 1 Hz or 5 Hz and the center modulation frequency is 90, 400, 800, or 900 Hz. The noise equivalent power is determined experimentally by measurin

the signal-to-noise ratio in a specified narrow electrical bandwidth called the measurement bandwidth. The value obtained for a known amount of radiant power is linearly extrapolated to the power that would give a signal to noise ratio of unity. The definition is given by:

$$P_n \equiv \mathcal{H} A \left(\frac{V_n}{V_s}\right) \frac{1}{\sqrt{\Delta f}} \qquad (55)$$

where $\mathcal{H}$ is the irradiance, A is the detector area and V_n/V_s is the ratio of the rms noise voltage in bandwidth Δf, to the rms signal voltage. The units are Watts/(Hertz)$^{1/2}$. Most detectors exhibit a noise equivalent power directly proportional to the square root of detector area. The <u>detectivity</u> is accordingly defined as:

$$D^* \equiv \frac{\sqrt{A}}{P_n} \qquad (56)$$

Definitions of (55) and (56) are concerned with detector response to blackbody radiation at a given temperature. For selective detectors, the response to monochromatic radiation may be quoted.

B. RESPONSIVITY.

This refers to the output signal per unit radiant power incident on the detector. It is measured in volts/watt and will be denoted by r. We have:

$$r = \frac{V_s}{P} = \frac{V_s}{\mathcal{H} A} \qquad (57)$$

It is seen from a comparison of Equation (57) with Equations (55) and (56) that the responsivity may be written in terms of noise equivalent power and detectivity as:

$$r = \frac{V_n}{P_n \cdot \sqrt{\Delta f}} = \frac{D^* V_n}{\sqrt{A \cdot \Delta f}} \qquad (58)$$

One may also specify the responsivity to monochromatic radiation, rather than to blackbody radiation.

C. MODULATION FREQUENCY RESPONSE.

This factor determines the changes in responsivity and detectivity of a detector as a function of the modulation (or chopping) frequency. In most applications, it is desired that the detector response be independent of modulation frequency, but this is not realized with practical detectors.

Semiconductors have a characteristic carrier recombination time. This limits the rapidity with which a detector will respond

to chopped radiation. At low modulation frequencies, the instantaneous carrier density follows the rise and decay of radiation upon the detector surface. At higher frequencies, this is no longer true and carrier generation may lag the rapid rise and fall of incident radiation. As a result, the responsivity is reduced. In general, the modulation frequency should be chosen such that:(25)

$$f \geq \frac{1}{2\pi\tau} \tag{59}$$

where τ is the carrier lifetime identical with detector response time. At a modulation frequency which corresponds to the equality in (59), the detectivity is maximum, whereas the responsivity is about 71% of its maximum value. If this modulation frequency is decreased, the responsivity is improved but detectivity is reduced, so that optimum conditions are represented by the equality (59).

D. MATHEMATICAL ANALYSIS OF BOLOMETERS.

The change in electrical resistance of a material on heating depends on the temperature coefficient of resistance defined by:

$$\alpha = \frac{1}{R}\frac{\partial R}{\partial T} \tag{60}$$

where R is the resistance at temperature T. From Equations (52) and (53) where the resistance of a metal and semiconductor are given as a function of temperature, we can evaluate α as:

$$\alpha = \frac{\gamma}{1+\gamma(T-T_o)} \qquad (61)$$

for a metal, and as

$$\alpha = -\frac{\beta}{T^2} \qquad (62)$$

for a semiconducting material. Also, in terms of a small change in temperature, the resistance change of either a metal or semiconductor is obtained from (60) as:

$$\Delta R = \alpha R . \Delta T \qquad (63)$$

In this analysis, the bolometer is assumed to be connected as in Figure 12, in series with a load resistor and a battery. Referring to Equation (46), the output signal resulting from a change in the resistance of the bolometer element, is given by:

$$\Delta V_L = V_o . \Delta R . \frac{R_L}{(R+R_L)^2} \qquad (64)$$

where the minus sign is disregarded. The bolometer element is subject to Joulean heating which results from the steady current supplied by the battery. Part of this heat is dissipated by conduction to the thermal sink and by radiation to the surroundings. The remainder serves to raise the temperature of the bolometer element, so that in the absence of radiation we have:

$$C\frac{dT}{dt} + \bar{K}(T-T_o) = I^2R \qquad (65)$$

where C is the heat capacity of the bolometer element and $\bar{K}$ is an average thermal conductance which governs the conductive and radiative heat flow to the surroundings at temperature T_o. Thus:

$$\bar{K}(T-T_o) = K_1 \epsilon \sigma (T^4 - T_o^4) + K_2 (T-T_o) \qquad (66)$$

where the first term on the right hand side denotes the radiative heat flow, and the second term denotes the conductive heat flow (usually to the thermal sink).(26)

When radiation falls on the bolometer, its temperature will be increased by an amount ΔT. If the incident radiant power is denoted by (P), we have from the heat transfer Equation (65) that:

$$C \frac{d(\Delta T)}{dt} + K \cdot \Delta T = \frac{d(I^2R)}{dT} \cdot \Delta T + P \qquad (67)$$

where (K) is the thermal conductance when the bolometer is at temperature $T+\Delta T$. The first term on the right hand side of the above equation is the incremental change in Joulean heating as a result of temperature rise. From the circuit of Fig. 12, we have:

$$\frac{d}{dT}(I^2R) = \frac{d}{dT}\left(\frac{V_o^2 R}{(R+R_L)^2}\right) = \frac{V_o^2 (R_L - R)}{(R_L+R)^3} \cdot \frac{dR}{dT} \qquad (68)$$

If we substitute the equivalent of dR/dT from Equation (60), into Equation (68), we get:

$$\frac{d}{dT}(I^2R) = \frac{V_o^2 R \alpha}{(R+R_L)^2} \cdot \frac{(R_L - R)}{(R_L+R)} \cdot \Delta T \qquad (69)$$

From Equation (65), we have for the steady-state $\frac{dT}{dt} = 0$, so that:

$$\bar{K}(T-T_o) = I^2 R \tag{70a}$$

or by writing the equivalent of I^2R from Fig. 12,

$$\bar{K}(T-T_o) = \frac{V_o^2 R}{(R+R_L)^2} \tag{70b}$$

Equation (70b) is now substituted into (69), giving:

$$\frac{d}{dT}(I^2R) = \alpha \bar{K}(T-T_o)\frac{R_L-R}{R_L+R}\cdot\Delta T \tag{71}$$

The heat transfer Equation (67) may now be written by substituting (71), as follows:

$$C\frac{d(\Delta T)}{dT} + K\cdot\Delta T = \alpha \bar{K}(T-T_o)\left(\frac{R_L-R}{R_L+R}\right)\Delta T + P \tag{72}$$

An effective thermal conductance is now defined from Equation (72) as:

$$K_e \equiv K - \alpha \bar{K}(T-T_o)\frac{R_L-R}{R_L+R} \tag{73}$$

With the above definition substituted in (72), the differential equation describing the behavior of bolometer becomes:

$$C\frac{d(\Delta T)}{dt} + K_e\cdot\Delta T = P \tag{74}$$

The solution of (74) may be obtained by assuming the input radiant power to be a periodic function of time.[27] This is valid when the radiation is modulated at a frequency (ω), as in a practical case. Then (P) may be described by:

$$P = P_o e^{j\omega t} \tag{75}$$

Under this assumption, the solution of (74) results in the following expression for the temperature increment:

$$\Delta T = \Delta T_o e^{-\frac{K_e t}{C}} + \frac{P_o e^{j\omega t}}{K_e + j\omega C} \tag{76}$$

The first term in (76) represents a transient which goes to zero with time if (K_e) is positive, and increases with time if K_e is negative. Thus, when K_e is negative, the bolometer overheats and burns up. If we refer to Equation (73), we see that overheating will occur when:

$$K < \alpha \bar{K} (T - T_o) \frac{R_L - R}{R_L + R} \tag{77}$$

since in such a case K_e would be negative. In practice, the load resistance (R_L) is taken much larger than the bolometer resistance R, and the thermal conductance (K) may be assumed to stay constant with temperature, i.e., $K \cong \bar{K}$. Equation (77) may be written in an approximate way by introducing the above assumptions. We have:

$$\bar{K} < \alpha \bar{K} (T - T_o) \tag{78}$$

or, the condition for unstable operation may be expressed as:

$$\alpha(T-T_o) > 1 \qquad (79)$$

which follows from (78). For thermister materials α is about 0.04. If the bias current is such that the bolometer attains a temperature of 325°K when the ambient is at 300°K, we have $\alpha(T - T_0) = 0.04\ (325 - 300) = 1$, so that the critical temperature of bolometer operated at room temperature is about 325°K. If the temperature is raised slightly above this by Joulean heating or heating due to the incident radiation, burnout will occur. For a metal bolometer, burnout will not occur even at very large temperatures. This fact may be illustrated by substituting the value of α for a metal (Eq. 61) into the unstability condition (79). We have:

$$\frac{\gamma(T-T_o)}{1+\gamma(T-T_o)} > 1$$ which never holds.

Under stable conditions when the transient term in Eq. 76 goes to zero, the absolute value of ΔT may be written as:

$$\Delta T = \frac{P_o}{\sqrt{K_e^2+\omega^2C^2}} \qquad (80)$$

By substituting the above, into Eq. 63, we can express the change in resistance of a bolometer element as:

$$\Delta R = \alpha R \cdot \frac{P_o}{\sqrt{K_e^2+\omega^2C^2}} \qquad (81)$$

The change in output voltage across the load may be expressed by substituting (81) into Equation (64). We then have:

$$\Delta V_L = \frac{V_o R_L}{(R+R_L)^2} \cdot \frac{\alpha R P_o}{\sqrt{K_e^2+\omega^2C^2}} \qquad (82)$$

The responsivity of the detector was defined as the ratio of output signal voltage to input radiant power. Using this definition, we can evaluate the responsivity from (82) simply by dividing both sides by the amplitude of incident radiant power P_o. Thus:

$$r = \frac{\Delta V_L}{P_o} = \frac{\alpha V_o}{\sqrt{K_e^2 + \omega^2 C^2}} \cdot \frac{R R_L}{(R + R_L)^2} \qquad (83)$$

When $R_L \gg R$ as in a practical case, the responsivity becomes:

$$r \approx \frac{\alpha V_o R}{R_L \sqrt{K_e^2 + \omega^2 C^2}} \qquad (84)$$

with $K_e \equiv K - \overline{K}(T - T_0)$ for large R_L, by Eq. (73). It is seen that the responsivity of a bolometer is proportional to the bias voltage and the ohmic resistance of the bolometer element. Although the bias voltage must be made large to get a large responsivity as seen from (84), this is practically not feasible since the bias current may then cause burnout, if the temperature limit imposed by (79) is exceeded. It should be indicated that (84) gives the responsivity of the bolometer element only. For a bridge circuit arrangement, the effective responsivity is one-half of this value.

The detectivity of a bolometer can be found from Eq. 58 which relates the detectivity of a detector to its responsivity. We have:

$$D^* = \frac{r \sqrt{A \cdot \Delta f}}{V_n} \qquad (85)$$

where Δf is the reference bandwidth, (A) is the detector area and (V_n) is the noise voltage of the detector. The noise mechanism in bolometers is thermal noise (or Johnson noise) due to the random motion of electrical charges in the material. The rms value of the noise voltage is given by:[28]

$$V_n = (4kTR.\Delta f)^{\frac{1}{2}} \qquad (86)$$

where Δf is the measurement bandwidth, and (k) is Boltzmann's constant equal to 1.38×10^{-23} joules/^{o}K. At room temperature, the value of $(4kT)$ is 16.7×10^{-21} joules. The corresponding noise voltage would be:

$$V_n = 1.28 \times 10^{-10}. (R.\Delta f)^{\frac{1}{2}} \qquad (87)$$

The noise voltage produced by a $(2\ M\Omega)$ thermistor detector flake operated at room temperature and chopped at 100 Hz would be 0.6 V in a 10 Hz bandwidth.[29] Detectivities are about 2×10^{8} $\frac{cm(Hz)^{1/2}}{watt}$ at 10 Hz chopping frequency. Responsivities obviously depend on the circuit connection, but values ranging from 40 volts/watt to 1065 volts/watt have been attained. These values are larger for thermistor bolometers equipped with a germanium lens.

VI. EXPERIMENTAL PREPARATION OF THERMISTOR MATERIALS

The vital part of a thermistor infrared detector is the active element which is known to be composed of a mixture of nickel, cobalt, and manganese oxides. These oxides are formed into approximately 10μ thick layers and mounted on a dielectric material with good heat conductivity. The resulting arrangement shows the characteristics of a semiconductor with resistances in the megohm range and a temperature coefficient of resistance as high as 0.04. For a (1 MΩ) thermistor flake, the resistance change per degree centigrade variation may be obtained from Equation (63). We have:

$$\Delta R = (0.04)(1\times10^{+6})\ \Omega/^{\circ}C$$

For an incident radiant power which changes the thermistor temperature by 10^{-4} degrees, the corresponding resistance change would be (4 Ω). This resistance increment is sufficient to disturb the balance of a Wheatstone Bridge Circuit arrangement so that the resulting signal may be recorded by a sensitive voltmeter.

A. VACUUM TECHNIQUES.

The writer considered the possibility of using vacuum techniques in the preparation of thermistor materials which would provide the thermal sensitivity indicated above. Due to the restrictions imposed on the thickness of active elements, the use of

chemical or electro-chemical techniques was not found feasible. Furthermore, it is not possible to deposit thin layers of thermistor materials on to non-metallic bases, by using electrochemical methods. However, in a vacuum coating unit, any metal or thermally stable compound may be evaporated on to metallic or dielectric bases with precise thickness control, with a minimum of dust contamination, and the resulting layer is sufficiently uniform for most purposes.

The advantage of evaporating a material in vacuum arises from the fact that the mean free path of vapour molecules increases with reduced atmospheric pressure. The mean-free-path is defined as the average distance travelled by a vapour molecule before colliding with gas molecules present in the environment. At an atmospheric pressure of 0.1μHg, the mean free path is about 45 cm., so that molecules of the vaporizing material are not likely to experience collisions with residual atmospheric constituents. As a result, vapor molecules propagate linearly and condense on a base material placed at a certain vertical distance from heated specimen and the collecting area is in the order of a mean-free path length.

During evaporation, electrical heating is supplied to a high melting point filament usually made of tungsten. It is necessary that the filament be inert to chemical reaction or alloy formation with the material to be evaporated. Furthermore, the melting point of the filament should exceed that of the evaporant. In practice, the choice of the type of filament to be used, as well as its shape depends on the nature of evaporant. If the evaporant is a

metal available in the form of a thin wire, it may be wound around the filament. For non-metallic evaporants, the filament is replaced by a boat-shaped metal holder which is selected so as to be inert to chemical reaction with the evaporant. Usually, such holders are made from tungsten, molybdenum, or platinum. Alumina crucibles may also be used in certain applications.

After the type, size, and shape of the filament or specimen holder are determined, the next problem is the adhesion of condensed vapor on to the collecting base or the substrate. Usually, a strong adhesion of a metallic film on to metallic substrates is readily achieved. For dielectric substrates such as sapphire, quartz, or glass which are encountered in infrared technology, the problem of adhesion depends on the evaporant used. In the following paragraphs, the vacuum deposition properties of thermistor materials will be discussed in order to establish the experimental procedure to be followed. The discussions are largely based on experiments conducted at Çekmece Nuclear Research Center with the Vacuum Deposition Plant described in the Appendix.

In general, two different methods are available for depositing thin films of metal oxides on to dielectric substrates. The relative merits of each method will be given with respect to the oxides of nickel, cobalt, and manganes.

B. DIRECT EVAPORATION OF THE OXIDES.

This process is complicated by the fact that chemical reactions may take place at high temperatures between the metal oxide, the heater material, or the residual gases in the vacuum chamber.

Usually, the metal oxide tends to decompose when the partial pressure of oxygen in the chamber becomes lower than that required for the stable existance of the compound. Nickel oxide (NiO) has a melting point of 2090°C but dissociates at 1596°C, at a vapor pressure of 10 Hg.[30] Similarly, manganese dioxide (MnO_2) decomposes at 535°C to form MnO and Mn_3O_4.[31] Cobalt oxide (CoO) has a melting point of 1800°C and also dissociates at reduced pressures around 10 μHg. Both NiO and CoO form the metal and liberate oxygen. In order to prevent dissociation, it is possible to deliberately establish a poor vacuum in the chamber, thus raising the partial pressure of oxygen above the critical level which causes dissociation. However, this will have a negative effect on film structure, as the resulting deposit will be contaminated and less uniform.

In a set of experiments using NiO, CoO, and MnO_2, various mixtures of these oxides in powder form, were evaporated at a vacuum pressure of 20 μHg. The dissociation of CoO and NiO to form the metal, was observed. The heater material was a thin foil of molybdenum formed into a boat-shaped holder. It was observed that the heater cracked at heating currents in excess of 200 amperes while the dissociated oxides were still in solid phase. Although a deposit was obtained, it contained poorly oxidized traces of manganese only, and was found to yield no response upon exposure to thermal radiation. In all experiments, it was impossible to evaporate the residual solids on the heater surface since the heater material invariably cracked before such constituents were melted. Theoretically, it is possible to obtain a highly oxidized deposit from NiO, CoO, and MnO_2 mixtures,

providing the dissociated oxides are baked in air at an average temperature of 400°C. It was however not possible in our experiments to verify this procedure due to heater material failures at temperatures necessary for the evaporation of dissociated constituents.

C. HEAT OXIDATION OF A METAL FILM.

An alternative procedure for obtaining metal oxide films is the vacuum deposition of the metal, which is then heated in the presence of air in order to be oxidized. At a vapor pressure of 10 Hg, the evaporation temperatures of Ni, Co, and Mn are respectively 1510°C, 1649°C, and 980°C. All of these metals may be evaporated from tungsten filaments if certain precautions are taken. Manganese does not form alloys with tungsten and may readily be evaporated. Nickel alloys with tungsten and may dissolve the filament at temperatures below 1500°C. To prevent alloy reaction, nickel should be evaporated rapidly. This is possible by quickly adjusting the heater current to high values. Cobalt should be evaporated in exactly the reverse manner. At temperatures below 1650°C, cobalt does not appreciably alloy with tungsten so that the heating current should be kept low when evaporating cobalt. It is further necessary that cobalt and nickel specimens be spread around the filament in order to prevent weight concentrations. This can be achieved by winding the evaporants around the filament, but the weight of the evaporant should not exceed 30% of that of the filament.(32), (33)

D. METHODS.

The following method was adopted in the preparation of samples by the heat-oxidation technique:

1. Cleaning of the Filament: A tungsten filament was available in the form of multi-loop wire. In order to remove dust and oxide contaminations on the filament, it was first heated to high temperatures in vacuum until a white, shiny surface was obtained.

2. Cleaning of the Substrate: Glass and quartz were used as the substrate material. Hand touch was avoided since the film structure is negatively effected by oily traces and dust particles on substrate. The substrate was first rubbed with a piece of cotton dipped into a solution of dilute HCl. It was subsequently rinsed with water and dried by applying cotton. In order to remove residual pieces of cotton on the surface, the substrate was then exposed to a fan-type dryer before being place in the coating unit.

3. Evaporation: The available constituents, nickel and cobalt, were evaporated from a tungsten filament. Due to the required small size of the film, only a small fraction of the vapor was allowed to condense on the substrate. It was therefore necessary to carry out at least 4 evaporations in order to obtain appreciable deposit buildup.

The coating unit available was not equipped with a mechanism for the measurement of deposit thickness. A preliminary series of experiments were therefore conducted to determine optimum thickness values by varying the weight of evaporant used. Very thin layers of metals were found to be transparent, especially on glass

substrates. Furthermore, the resistances measured for such layers did not reveal the properties of the bulk material used.

In the preparation of final samples, optimum conditions were utilized in order to deposit a layer with high resistance and small area. In general, heat oxidation of metal mixtures obtained by depositing nickel and cobalt with successive evaporations, proved to worsen the film structure and reduced the thermal response obtained. Therefore, mixtures were avoided. A description of finished samples will be found in the appendix.

4. Heat Oxidation: A "Muffle Furnace" available at the R.C. Metallography Laboratory was used to oxidize metal films. The furnace may be adjusted to any temperature up to 1000°C and provides electrical heating from an array of filaments facing each other. In order to avoid dust settlement on the film, the samples were shielded with a heat resistant glass. In principle, oxidation rate decreases with increased film thickness. For the samples prepared, a heating time of 2 hours was found necessary, at 400°C.

5. Ohmic Contacts: Very thin sheets of copper were cut and glued on to the substrate with epoxy resin. Depending on the chosen area of the deposit, a layer was deposited between these leads, but not in contact with them. Electrical connection between the deposit and copper terminals was then provided by evaporating a layer of gold on to the terminals and also on part of the deposit edges. The use of copper terminals makes soldering possible for use in an external circuit. Gold layer provides a smooth transition between the deposit and the terminals and also prevents oxidation of copper.

VII. CONCLUSIONS

A study of the processes by which infrared radiation is generated and transmitted, shows that, the efficiency of an infrared detection system will depend on the following:

1. The radiant intensity of source emission and its distance from the detector. The intensity was seen to be determined by the temperature of the source as well as the emissivity of its surface, and may be expected to decrease as the inverse square of distance between the source and detector.

2. The interferences presented by background radiation in the wavelengths to be detected. Background radiation was shown to be composed mainly of solar radiation and infrared emission from the terrain. These interferences are naturally minimized within a wavelength band between 3.0μ and 6.0μ. Source temperatures that will give rise to maximum emission within the above limits, range from about 1000^{o}K to about 500^{o}K.

3. Behavior of the atmosphere at infrared wavelengths of interest. It was seen that the atmosphere provides a number of absorbtion regions along with a few convenient transmission regions. Infrared radiation will in general be exponentially attenuated through the atmosphere, the degree of attenuation being a function of weather conditions and mainly the CO_2 and water vapor constituents present at a given altitude.

4. A carefully designed optical system that will serve to filter out background effects and also enhance the amount of incident radiant power by a good focusing arrangement. The choice of lenses, filters, and window materials for this purpose, will be based upon a comparison of infrared transmission characteristics of available materials. Other important criteria in optical materials are the index of refraction and thermal and mechanical strength.

With respect to the types of detectors, it may be concluded that photon detectors are characterized by a wavelength-dependent sensitivity and a fast speed of response. In contrast, thermal detectors are characterized by a practically constant sensitivity over the spectrum, and a comparatively slow speed of response. Photon detectors should be preferred for near and intermediate infrared regions. The minimum radiant power that may be processed by any detector will depend on the noise signal output from the detector.

A combination of precise solid-state and vacuum techniques is necessary for the construction of sensitive elements. It is observed that the search for new materials suitable for thermal detection has been rather slow. The use of vacuum deposition methods for preparing bolometer flakes, was seen to present the following difficulties:

1. Ordinary Coating Units are designed for depositing very thin, transparent layers with a thickness not exceeding 1.0μ. This is a serious limitation on the required thicknesses of thermistor flakes (about 10μ).

2. The vacuum-evaporation characteristics of common thermistor materials impose special conditions on the type of Coating Unit. A "Flash Evaporation" arrangement should be designed for evaporating the oxides of nickel, cobalt, and manganese. This arrangement provides for a continuous flow of evaporant on to a heated source in vacuum. Evaporation is largely assisted since small particles fall on a very hot source material.

3. Very thin deposits are invariably transparent, and a certain thickness should build up in order that the deposit may exhibit the electrical characteristics of evaporant or bulk material. A method for measuring the deposit thickness is therefore essential.

Providing the above problems are solved, it is possible to experiment on thermistor materials by using vacuum apparatus. Undesirable chemical reactions may be minimized by following the procedures outlined in the previous section. Unless the apparatus is not equipped with means to enable direct evaporation of oxides, the heat oxidation method should not be utilized. Deposits are largely contaminated, and the layer is not uniformly oxidized in this method. A subject which requires extensive research is the necessity of providing a thermally conductive layer in between the deposit and the substrate. This will greatly enhance the speed of response of a thermal detector.

It is hoped that future experimenters in the field of infrared detection will find the contents of this work useful for an introductory purpose.

APPENDIX

A. DESCRIPTION OF SAMPLES

Sample:1

Substrate: Flat circular glass of 28 mm diameter and 1.5 mm thickness.

Active Material: Pure metallic nickel.

Active Area: 5mm x 4mm

Sample:2

Substrate: Flat rectangular quartz crystal of dimensions 18mm x 14mm and thickness 1.5 mm.

Active Material: Pure metallic nickel.

Active Area: 5.5mm x 3.5mm

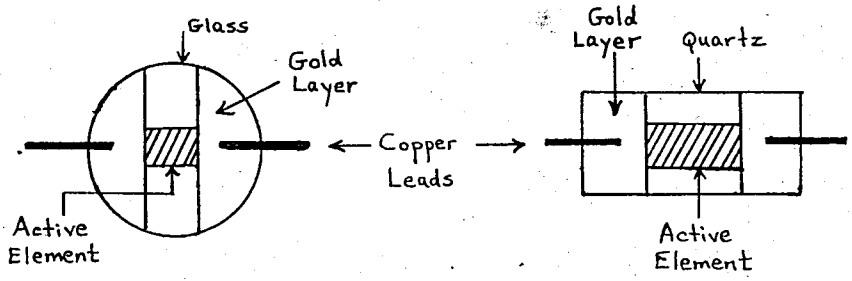

Sample : 1 Sample : 2

Common Experimental Conditions:

Total Weight of nickel: 10 gm.

Total Evaporation Time: 6 min.

Average Vacuum Pressure: 30 μHg

Average Heating Current: 150 Amp.

Type of Heater Material: Tungsten Filament

Total Weight of Gold: 3 gm

Type of heater material for gold: Molybdenum Boat

Heat Treatment: Prolonged oxidation at low temperatures, near 100°C.

Remarks:

In order to prevent the melting of the epoxy used in fixing the ohmic contacts to the substrate, it was necessary to avoid high temperatures during heat oxidation. During preliminary experiments on samples without ohmic contacts, the necessary oxidation time was found to be about two hours at 400°C. With a furnace temperature of 100°C, the corresponding oxidation time will be much longer. In our samples, it was observed that a heating time of 24 hours at 100°C introduced a small degree of oxidation as evident from the change in the resistance of the samples at room temperature. The resistance of each sample was 6 ohms in metallic state and about 12 ohms after heat treatment, for 24 hours at 100°C. It may be concluded that the rate of oxidation is sharply reduced at low temperatures, and with the electrode technique used in our experiments, it is very difficult to apply an effective heat treatment. As a result, the samples are in fact metal bolometers rather than thermistor bolometers. The resistance values obtained, agree with commercial nickel strip bolometers, but the responce times are much longer in our samples. Reasons for this behavior are explained in the previous sections.

B. MEASUREMENTS ON SAMPLES

1. Resistance-Temperature Characteristics: Since the samples are in metallic state, their resistances will vary linearly with temparature. In order to determine the temparature coefficient of resistance, the samples were successively heated in a furnace, with the ohmic contacts connected to an impedance bridge, thus enabling simultaneous readings of temperature and resistance.

Values of resistance measured for a range of temperatures up to 160°C are tabulated below, and the data is plotted on the next page.

T (°C)	20	40	60	80	100	120	140	160
R_1 (ohms)	10.8	11.1	11.5	12.0	12.4	12.8	13.1	13.5
R_2 (ohms)	10.3	10.7	10.9	11.2	11.6	11.9	12.2	12.5

In order to determine the slope of each R-T curve, the points A', B' and A, B are chosen for samples 1 and 2 respectively. the coordinates of these points are: A' (66°C, 11.65 ohms), B' (145°C, 13.3 ohms), A (65°C, 11.05 ohms), B (150°C, 12.4 ohms).

Thus for sample:1, we have,

$$\gamma_1 = \frac{1}{R_o} \cdot \frac{\Delta R}{\Delta T} = \frac{1}{11.65} \cdot \frac{13.3 - 11.65}{145 - 66} = 0.0018/°C$$

Similarly, for sample:2, we get,

$$\gamma_2 = \frac{12.40 - 11.05}{150 - 65} \cdot \frac{1}{11.05} = 0.0015/°C$$

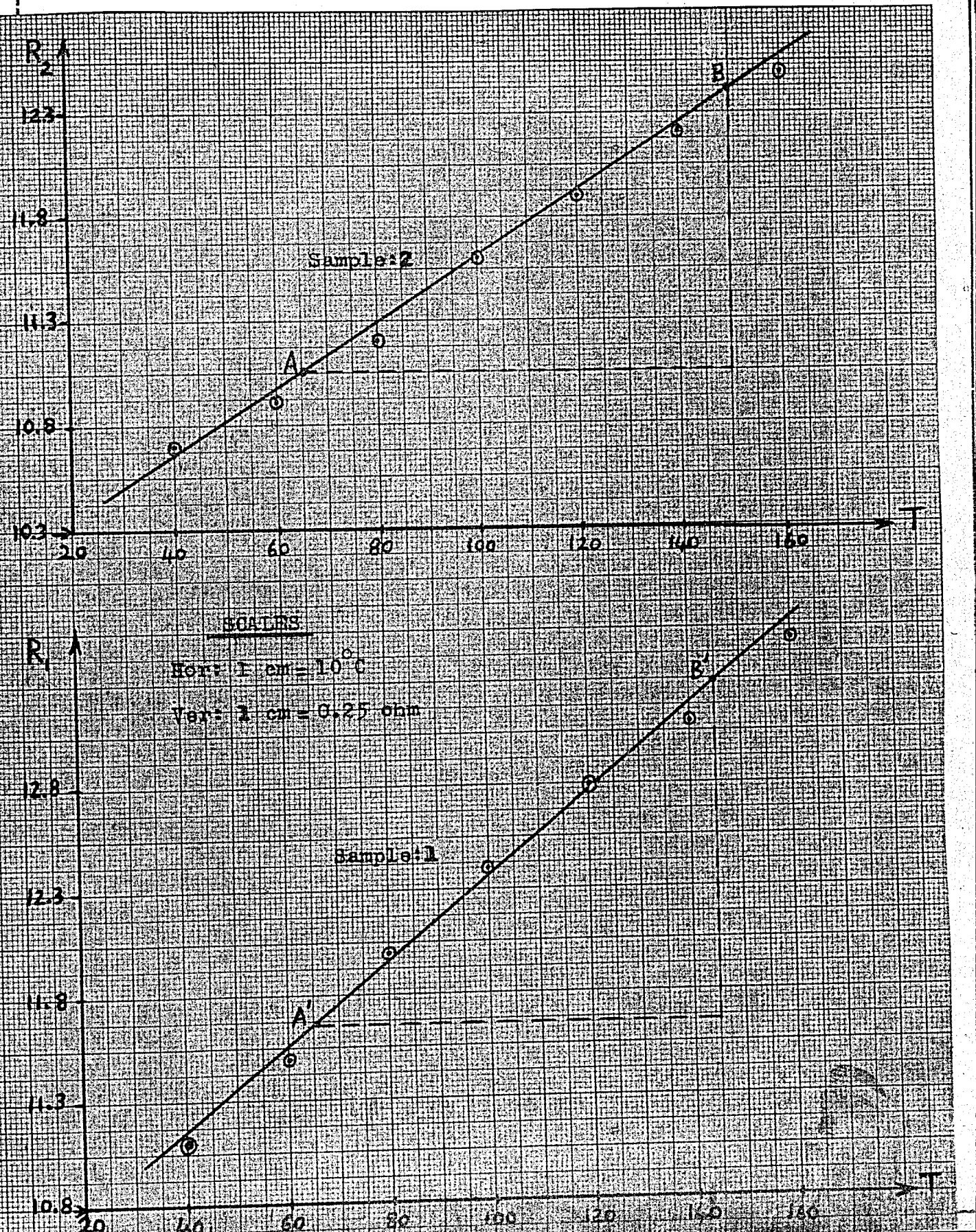
R2
12.3
11.8
11.3
10.8
10.3
Sample:2
A
B
20
40
60
80
100
120
140
160
T
SCALES
Hor: 1 cm = 10° C
Ver: 1 cm = 0.25 ohm
R1
12.8
12.3
11.8
11.3
10.8
Sample:1
A'
B'
20
40
60
80
100
120
140
160
T

The accepted value of γ for nickel, is 0.0033. The discrepancy in our result is probably due to the impurities introduced during evaporation of the metal and the heat treatment. Gold contacts will not reduce the value of γ since gold is known to have a higher temparature coefficient of resistance than nickel.

2. Detection range and NEP : To establish an order of magnitude for the detection range of the samples, the following setup was used:

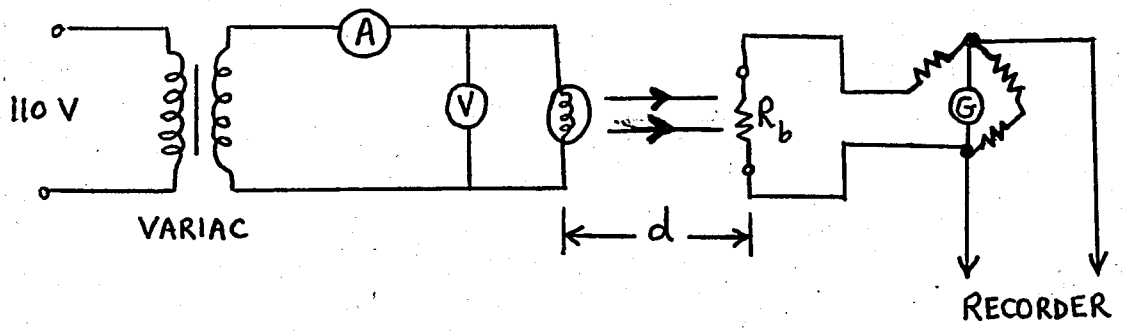

The minimum deflection in the bridge that can be read by the recorder is 200 μV. The infrared lamp was adjusted to its maximum range , and dissipated 880 W at a distance d from the sample. For values of d greater than 50 cm , there was no output from either sample, readable on the recorder. The Nep of each sample under DC exitation would then be given by:

$$P_n = \gamma A_d = \frac{P_o}{2\pi d^2} A_d$$

where A_d is the sensitive area, P_o is the power emitted by the lamp. If we assume that the lamp emits all the power dissipated in its filament, $P_o = 880$ W. The detector area $A_d = 20\ ^{mm^2}$ for each sample, and with d = 50 cm, we get:

$$P_n = \frac{880 \times 20 \times 10^{-2}}{6.28 \times (50)^2} = 1.12 \times 10^{-2}\ W$$

The detectivity may thus be determined from $D^*=\sqrt{A_d}/P_n$ as,

$$D^*=4\times10^2 \text{ cm/W}$$

The value of detectivity for sensitive commercial bolometers measured through AC exitation is about 2×10^8.cm/W.

3. Measurement of Response Time: The rise and decay of signal voltage from the samples is shown in the following graphs plotted by the recorder. In this experiment, the infrared lamp was placed '30' cm from the samples, and was switched off suddenly, after a certain level of the signal voltage. As seen from the graphs, the sample cooled of exponentially. The signal variation after switch-off, may be represented by,

$$V=V_o e^{-t/\tau}$$

where V_o is the value of signal voltage just before switch-off, t denotes time, and τ is the time constant of the decay. The time constant is the time required to obtain a signal voltage of 37% of the initial value, as seen by putting $t=\tau$ in the above expression. The initial voltage before switch-off, is 1.43 mV for sample 1, and 1.50 mV for sample 2. Accordingly, τ is defined as the time required to have a signal of 0.53 mV for sample 1 and 0.55 mv for sample 2. These values of τ as shown in the following graph, are:

$$\tau_1 = 86 \text{ sec}$$

$$\tau_2 = 84 \text{ sec}$$

The value of τ for a good bolometer would be in the order of a few milliseconds. Both D^* and τ may be improved by utilizing a much more effective conduction to the substrate. These points require further experimentation.

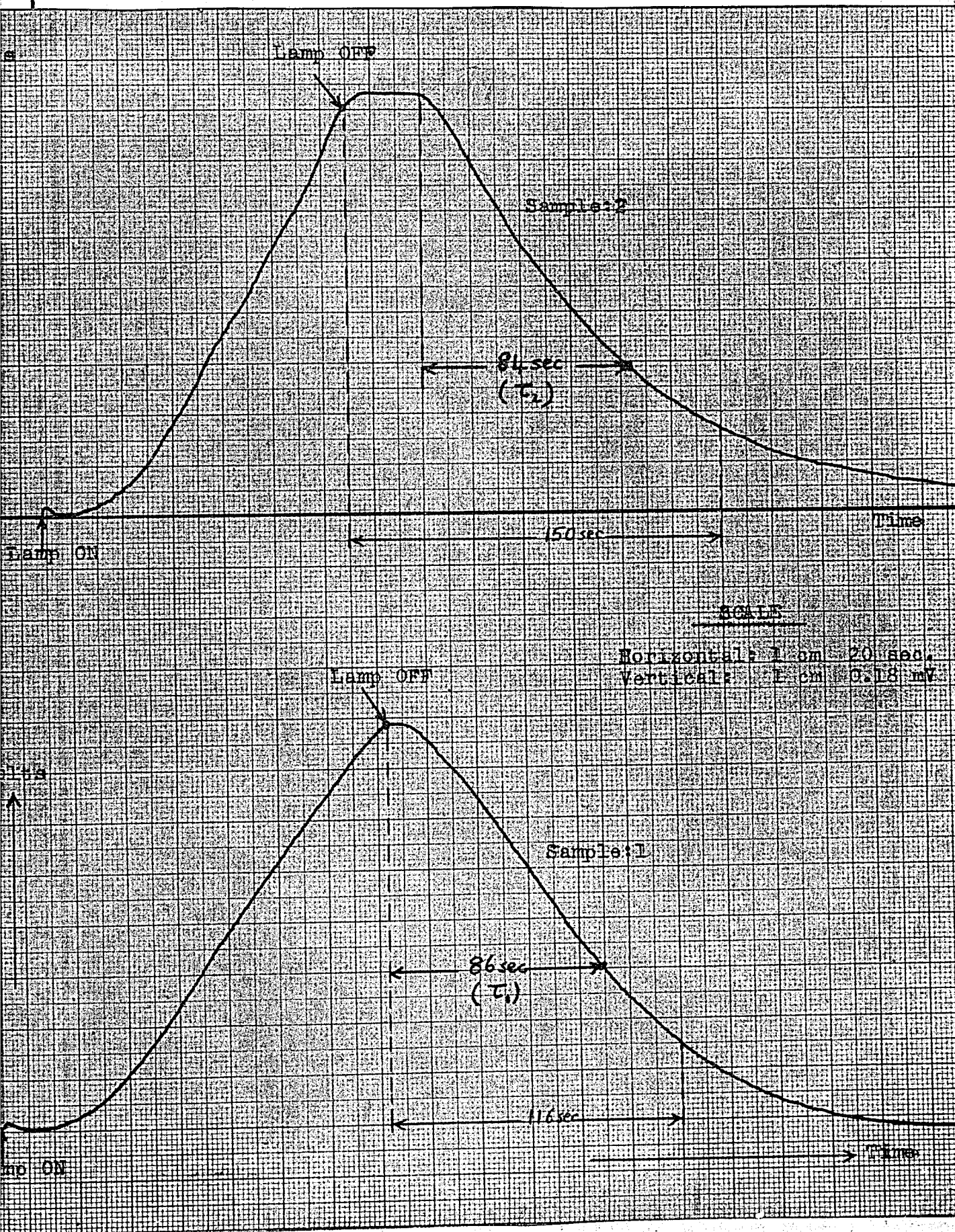
Lamp OFF
Sample:2
84 sec
(τ2)
Lamp ON
150 sec
Time
SCALE
Horizontal: 1 cm 20 sec.
Vertical: 1 cm 0.18 mV
Lamp OFF
Sample:1
86 sec
(τ1)
116 sec
Time

C. DESCRIPTION OF THE VACUUM COATING UNIT

The Vacuum Coating Unit at the Experimental Physics Division, Çekmece Nuclear Research Center, is seen below. This Unit is designed for applications of an optical nature, mainly the deposition of aluminum films on mirrors, and various antireflection coatings. The specifications are as follows:

Manufacturer: Edwards High Vacuum Ltd., Crawley, Sussex, England.

Model : Speedivac

Operation Mode: Rotary Pump and Oil Diffusion Pump.

Chamber Size: About 30 cm diameter.

Ultimate Vacuum Level Possible: 1.0 microns Hg.

Maximum Heating Current: 400 Amp.

Average time required to establish vacuum: About 0.5hr after turn on.

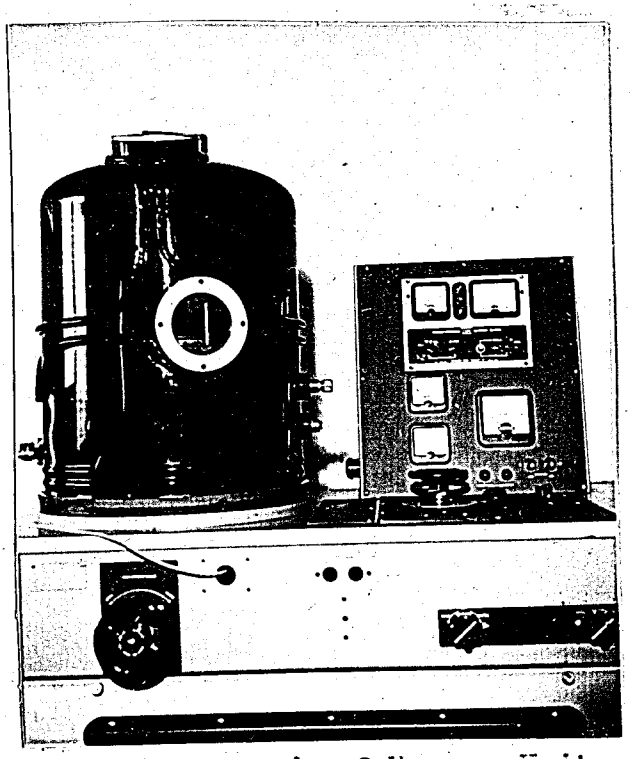

Photograph of Vacuum Unit

D. PHYSICAL CONSTANTS

Velocity of light in free space, c	3×10^{8} m/sec
Planck's constant, h	6.63×10^{-34} joule.sec
Boltzmann constant, k	1.38×10^{-23} joule/K
Stefan-Boltzmann constant, σ	5.67×10^{-8} watts.m^{-2}.K^{-4}
Charge on an electron, e	1.60×10^{-19} coulomb
Mass of an electron, m	9.11×10^{-31} kg
Standard Atmosphere	760 mm Hg
Electron-volt unit	1.6×10^{-19} joule
Micron unit	1.0×10^{-6} m
Angstrom unit	1.0×10^{-10} m
Absolute temperature scale, ^{o}K	273.2 + ^{o}C

E. WORK FUNCTİON (ϕ) OF MATERIALS [34]

Unit: eV

MATERIAL	ϕ	MATERIAL	ϕ	MATERIAL	ϕ
Lithium Li	2.39	Boron B	4.50	Arsenic As	5.11
Sodium Na	2.27	Aluminum Al	3.74	Antimony Sb	4.08
Potassium K	2.15	Gallium Ga	3.96	Bismuth Bi	4.28
Rubidium Rb	2.13	Titanium Ti	4.09	chromium Cr	4.51
Cesium Cs	1.89	Molybdenum Mo	4.27	Zirconium Zr	3.84
Copper Cu	4.47	Hafnium Hf	3.53	Tungsten W	4.50
Silver Ag	4.28	Thorium Th	3.41	Uranium U	3.74
Gold Au	4.58	Carbon C	4.39	Selenium Se	4.72
Calcium Ca	2.76	Silicon Si	4.10	Manganese Mn	3.95
Strontium Sr	2.35	Germanium Ge	4.56	Iron Fe	4.36
Barium Ba	2.29	Tin Sn	4.11	Cobalt Co	4.18
Magnesium Mg	3.46	Lead Pb	4.02	Nickel Ni	4.84
Zinc Zn	3.74	Vanadium V	4.11	Rhodium Rh	4.65
Cadmium Cd	3.92	Cebium Cb	3.99	Paladium Pd	4.82
Mercury Hg	4.52	Tantalum Ta	4.12	Iridium Ir	4.57
Beryllium Be	3.37	Tellerium Te	4.73	Platinum Pt	5.29

F. ENERGY GAP VALUES FOR SELECTED SEMICONDUCTORS AT ROOM TEMPARATURE

Unit:eV

MATERIAL	E_g	MATERIAL	E_g	MATERIAL	E_g
Diamond	6.00	Si	1.10	Ge	0.70
Sn	0.08	InSb	0.18	InAs	0.33
InP	1.25	GaAs	1.40	AlSb	1.65
InSe	1.00	GaP	2.25	Mg_3Sb_2	0.82
Ca2Si	0.90	Ca_2Sn	0.90	Ca_2Pb	0.46
ZnSb	0.56	GaSb	0.78	PbS	0.35
PbSe	0.27	PbTe	0.30	CdS	2.42
CdSe	1.74	CdTe	1.45	ZnSe	2.60
AgI	2.80	Ag_2Te	0.17	Cu_2O	2.10
Mg_2Si	0.70	Mg_2Ge	0.70	Mg_2Sn	0.30
ZnO	3.30				

REFERENCES

(1) Hackforth, H.L. Infrared Radiation. New York: McGraw Hill, 1960. P. 5.

(2) Smith, R.A., Jones, F.E., and Chasmar, R.P. The Detection and Measurement of Infrared Radiation. London: Oxford, 1960. P. 308.

(3) Sachs, M. Solid State Theory. New York: McGraw Hill, 1963. P. 154.

(4) Kruse, P.W; McGlauchin, L.D.; and McQuinstan, R.B. Elements of Infrared Technology. New York: Wilsy, 1962. Pp. 52-53.

(5) Eltro GmbH. Allgemeines über Infrarot. Heidelberg, February 1969. P. 11.

(6) Kruse, op. cit. P.31.

(7) Smith, op. cit. P.32.

(8) Hackforth, op. cit. P. 37.

(9) Kruse, op. cit. P. 76.

(10) Hackforth, op. cit. P. 41

(11) Ibid. P. 43.

(12) Simon, I. Infrared Radiation. Princeton: Van Nostrand, 1966. P. 21.

(13) Kruse, op. cit. P. 73.

(14) Hackforth, op. cit. P. 63.

(15) Eltro GmbH, op. cit. P. 10.

(16) Kruse, op. cit. P. 143.

(17) Ibid. Pp. 159-160.

(18) Hackforth, op. cit. P. 109.

(19) Van der Ziel, A. Solid State Physical Electronics. Englewood Cliffs: Prentice-Hall, 1968. P. 209.

(20) Kruse, op. cit. Pp. 297-298.

(21) Ibid. P. 310.

(22) Barnes Engineering Company. "Thermistor Infrared Detectors." Bulletin 2-100, Stamford, Massachusetts, U.S.A. P. 3.

(23) Smith, op. cit. P. 61.

(24) Kruse, op. cit. P. 422.

(25) Ibid. P. 276.

(26) Smith, op. cit. P. 96.

(27) Kruse, op. cit. P. 347.

(28) Ibid. P. 238.

(29) Barnes Engineering Co., op. cit. P. 5.

(30) Holland, L. Vacuum Deposition of Thin Films. London: Chapman and Hall, 1961. Pp. 446-447.

(31) Ibid. P. 515.

(32) Ibid. P. 111.

(33) Ibid. P. 178.

(34) Angrist, S. W. Direct Energy Conversion. Boston: Allyn and Bacon, 1965.

BIBLIOGRAPHY

Barnes Engineering Co. "Thermistor Infrared Detectors." Bulletin 2-100, Stamford, Massachusetts, U.S.A.

Bender, H. Enfrary Işınlar. Ankara: E. U. Basımevi, 1959. M.M.V. İlmî İstişare ve Geliştirme Yayınları, No. 35-HAG-17.

Eltro GmbH. Allgemeines über Infrarot. Heidelberg, February 1969.

Hackforth, H. L. Infrared Radiation. New York: McGraw Hill, 1960.

Hass, G. (editor). Physics of Thin Films. New York: Academic Press, 1963.

Holland, L. Vacuum Deposition of Thin Films. London: Chapman and Hall, 1961.

Kruse, P. W.; McGlaunchin, L.D.; McQuinstan R. B. Elements of Infrared Technology. New York: Wiley, 1962.

Martin, A. E. Infrared Instrumentation and Techniques. London: Elsevier, 1966.

Neuringer, L. J. "Infrared Fundamentals and Techniques," Electrical Manufacturing. (March, 1960), Article 15.

Roberts, J. K. Heat and Thermodynamics. London: Blackie and Sons, 1940.

Sachs, M. Solid State Theory. New York: McGraw Hill, 1963.

Simon, I. Infrared Radiation. Princeton: Van Nostrand, 1966.

Smith, R. A.; Jones, F. E.; Chasmar, R. P. The Detection and Measurement of Infrared Radiation. London: Oxford, 1960.

Tuerk, F. E. "The Nature of Infrared," RCAF Observer. (July 3, 1964), Vol. 10, No. 3.

Van der Ziel, A. Solid State Physical Electronics. Englewood Cliffs: Prentice-Hall, 1968.